AN ABSTRACT OF THE THESIS OF

JOSEPH SHELDON BOTTERO for the MASTER OF SCIENCE
(Name) (Degree)

in OCEANOGRAPHY presented on 3 October 1968
(Major) (Date)

Title: AN ANALYSIS OF UPWELLING OFF THE SOUTHEAST ARABIAN COAST DURING THE SUMMER MONSOON

Redacted for Privacy

Abstract approved: _____
Robert L. Smith

A method is described for determining the absolute dynamic topography of the sea surface. Using hydrographic and wind data obtained in 1963, the surface topography and the horizontal and vertical mass transports off the southeast Arabian coast during the summer monsoon are calculated. As indicated by the calculations, upwelling occurs throughout a region extending at least 400 km offshore and paralleling the Arabian coast for over 1000 km. Upwelling is most intense in a narrow band adjacent to the coast. Because of the great breadth of the upwelling zone, the upwelled water is supplied from levels considerably deeper than those observed elsewhere in coastal upwelling areas.

An Analysis of Upwelling off the Southeast Arabian Coast During the Summer Monsoon

by

Joseph Sheldon Bottero

A THESIS

submitted to

Oregon State University

in partial fulfillment of
the requirements for the
degree of

Master of Science

June 1969

APPROVED:

Redacted for Privacy

Assistant Professor of Oceanography

in charge of major

Redacted for Privacy

Head of Department of Oceanography

Redacted for Privacy

Dean of Graduate School

Date thesis is presented 3 October 1968

Typed by Clover Redfern for Joseph Sheldon Bottero

ACKNOWLEDGMENTS

I would like to express my sincere appreciation to Dr. Robert L. Smith for his guidance and encouragement in the writing of this thesis.

I am indebted to Dr. C. N. K. Mooers for substantial contributions to this work. Much of Chapter III, Transport Equations, appeared originally in an unpublished note by Dr. Mooers.

Appreciation is extended to Dr. June Patullo for her critical review of the manuscript.

I am especially indebted to Mr. Carl Schaniel of the Naval Weapons Center, who encouraged me to return to school after a lapse of several years and who helped make it possible for me to do so.

TABLE OF CONTENTS

LIST OF TABLES

LIST OF FIGURES

Figure Page

AN ANALYSIS OF UPWELLING OFF THE SOUTHEAST ARABIAN COAST DURING THE SUMMER MONSOON

I. INTRODUCTION

Most of the world's major upwelling regions are located on the eastern sides of the oceans. Two notable exceptions, however, occur in the northern Indian Ocean, where upwelling takes place each summer along the Somali coast and off the southeast coast of Arabia. During the summer of 1963 the Arabian upwelling region was surveyed intensively by the Royal Research Ship Discovery (U. K.), as part of the International Indian Ocean Expedition. The present study is based on the Discovery data.

Figure 1 shows the western half of the Arabian Sea. The surface currents of the Arabian Sea are strongly influenced by weather factors and show seasonal reversals. There are two major wind systems in this part of the Indian Ocean: the Northeast Monsoon during winter, and the Southwest Monsoon during summer. In winter, under the influence of the Northeast Monsoon, the surface flow adjacent to the Arabian coast is toward the southwest. During summer, following the wind, this current reverses direction and flows toward the northeast. Little is known about the subsurface circulation. According to Rochford (1964), warm saline water from the Red Sea passes north of Socotra at a depth of about 800 m and spreads eastward and southward.

Rochford also found (1966) indications of a northward flow of antarctic intermediate water near 600 m, to the east of Socotra. These results were based on analyses of observed salinity distributions.

During the Discovery expedition (June through August, 1963) measurements of surface and subsurface velocities were made off the Arabian coast with suspended current meters and neutrally buoyant floats (The Royal Society, 1963). The surface currents were found to be mostly toward the northeast near the coast, and toward the southeast farther offshore. The subsurface measurements were not conclusive. Salinity, temperature, oxygen, and phosphate data indicated extensive upwelling close to shore. Here, as in other coastal upwelling areas, vertical motion can be explained as a response to a wind-caused divergence in the upper 100 m. From May through August the prevailing winds are southwesterly and nearly parallel to the coast. Under the action of these winds large quantities of water are transported offshore in the surface layer. Upwelling occurs as these waters are replenished from below.

II. DESCRIPTION OF THE METHOD

The results of the present study are given in Chapter VI. The numbers that appear there were obtained with the aid of an analysis technique first described by Wyrtki (1963). This technique utilizes hydrographic data and produces information about the absolute topography of the sea surface. It is based on a continuity argument. The oceanic region under consideration is divided into a number of closed, contiguous cells, and a requirement is made that the mass of water entering each cell equal the mass leaving. An historical antecedent is Stommel's (1958) treatment of the North Atlantic circulation in which he required the net transport across a line of latitude, integrated across the ocean, to vanish. The approach taken here is somewhat finer-grained, but is basically similar. In general, Wyrtki's method is valid wherver the flow is geostrophic with an Ekman component in the surface layer. Two types of input are necessary: hydrographic data, and wind observations. The hydrographic casts should reach a depth at which vertical motion is negligible. Figure 1 shows the hydrographic stations used in the present analysis.

Let S be a fixed, closed, simple curve on the surface of the ocean, and let S' be its projection on the ocean floor (see Figure 2). We will be concerned with mass transports into a cell bounded by the ocean surface, SS', and the ocean floor.[1] Let v_n be the

[1] SS' is the vertical, cylindrical surface extending from S to S'.

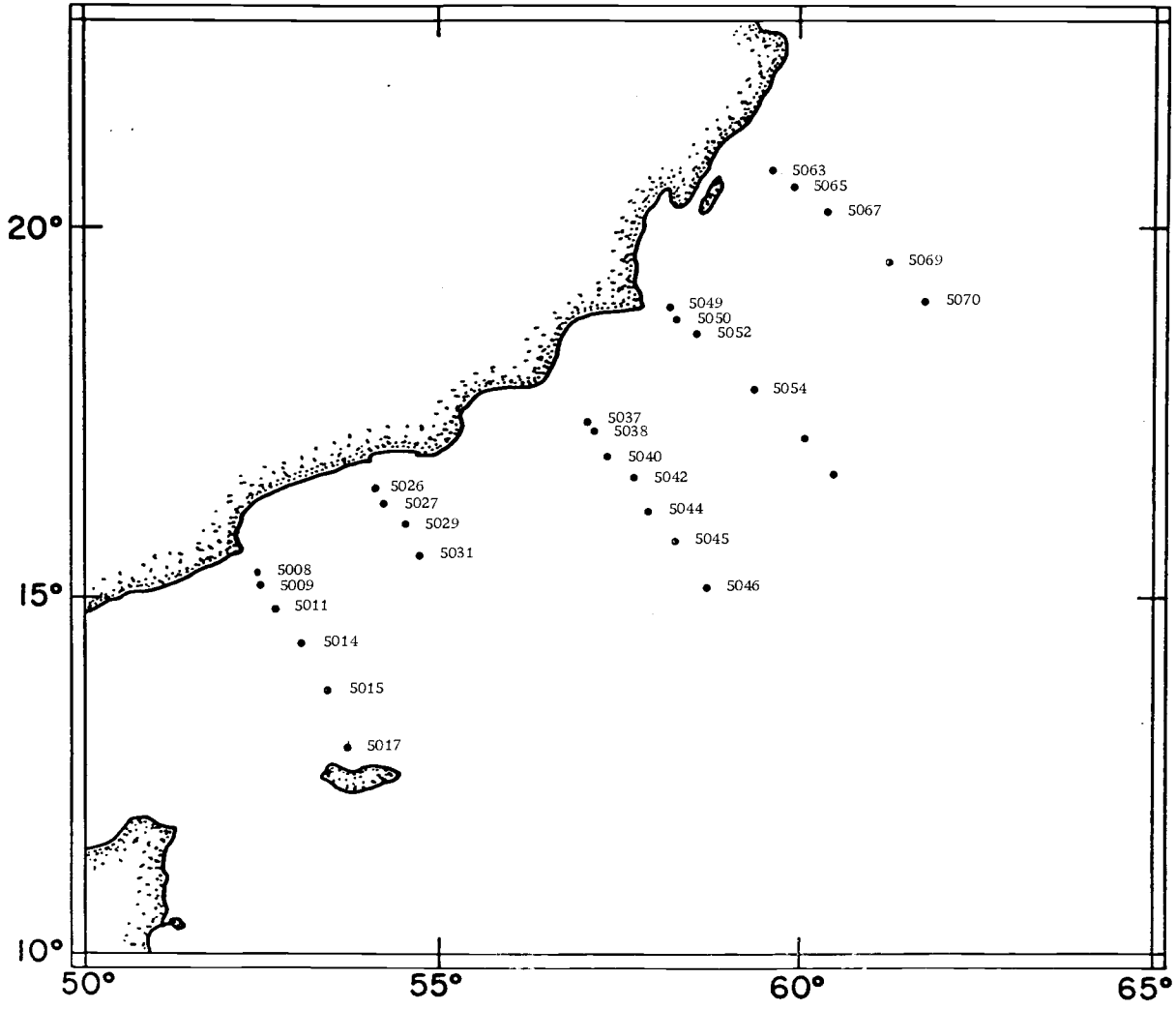

Figure 1. The western Arabian Sea, showing stations occupied by R. R. S. Discovery during June and July of 1963.

component of velocity normal to SS' (positive into the cell), let ρ be the density of the water, and let z be vertical distance measured positive upward. The horizontal mass transport into the cell is

$$T = \int_{S'}^{S} \oint_{S} \rho v_n \, dS dz \tag{1}$$

It will be assumed that the flow is approximately geostrophic, with a wind-induced component in the upper layer. Under this assumption, v_n is given by

$$\rho f v_n = - \frac{\partial p}{\partial S} + \frac{\partial \tau_s}{\partial z} \tag{2}$$

where f is the coriolis parameter, p is the pressure, and τ_s is the shear stress in the direction of S (positive clockwise around S). If evaporation and rainfall are slight or balance each other, no significant amount of water enters or leaves the cell at the sea surface. In addition, since S' lies on the ocean floor, no water passes through the bottom of the cell. Because a steady state has been assumed, conservation of mass then requires that $T = 0$. This requirement will appear below as a boundary condition.

The pressure gradient of Equation 2 has two parts, one related to the baroclinicity of the water column, and the other to the slope of the sea surface. Let h be the height of the sea surface, relative to an appropriate geopotential reference plane. Then

$$\left.\frac{\partial p}{\partial S}\right|_{z=\hat{z}} = \frac{\partial}{\partial S}\int_{\hat{z}}^{h} \rho g dz$$

$$= g\int_{\hat{z}}^{h} \frac{\partial \rho}{\partial S} dz + \rho g \left.\frac{\partial h}{\partial S}\right|_{z=h} \qquad (3)$$

The first term on the right-hand side of Equation 3 can be calculated from hydrographic data, but the second term contains $\partial h/\partial S$, which ordinarily is not known. If Equations 2 and 3 are substituted into Equation 1 and T is set equal to zero, the resulting expression contains only one unknown function, $\partial h/\partial S$. Under certain conditions this expression ($T=0$) uniquely determines $\partial h/\partial S$ along S. Ways of solving $T = 0$ for $\partial h/\partial S$ will be discussed in this chapter and Chapters III and IV. Once $\partial h/\partial S$ is known, horizontal velocities can be calculated from Equations 2 and 3.

In practice, hydrographic data are not continuous and the smoothly curved cell boundary of Figure 2 must be replaced by a polygonal structure. Given a sufficiently dense network of hydrographic casts, the ocean can be divided into a collection of three- and four-sided prisms whose vertices are located at hydrographic stations. A three-sided example is shown in Figure 3. Figure 4 shows an array of polygonal cells, viewed from above.

Consider Figure 3. Since A, B, and C of Figure 3 are hydrographic stations, ρ is available as a function of depth along AD,

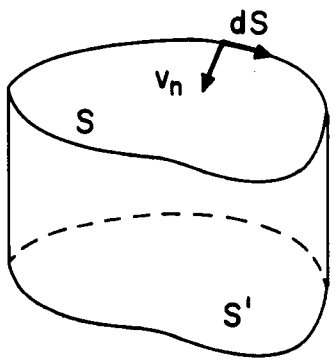

Figure 2. A cell formed by projecting a closed curve S at the sea surface onto the ocean floor.

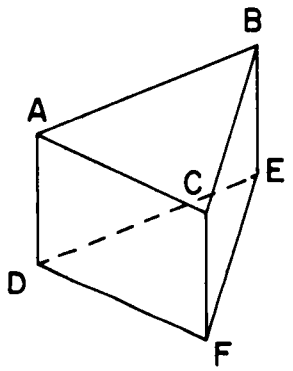

Figure 3. A 3-sided cell extending from the sea surface (ABC) to the ocean floor (DEF). A, B, and C are hydrographic stations.

BE, and CF. It will be assumed that ρ varies linearly between stations, so that the interstation velocities[2] can be computed by the standard dynamic heights method. There are several ways of determining $\partial h/\partial S$ along the periphery of a three-sided cell. We will rely primarily on a technique that requires that the slope along one side of the cell be known in advance. Given the slope along one side, the remaining two slopes can be adjusted to meet the condition $T = 0$.

Suppose then that the slope along AB of Figure 3 is given, and that the vertical density distributions beneath A, B, and C are known, together with the wind stress at the sea surface. The net transport into the cell depends only on the wind stress, the sea surface slopes between the three stations, and the density of the water along AD, BE, and CF. Of these, only the slopes between B and C and between A and C are not known. Since the height of B relative to A is given, the two unknown slopes can be calculated if the height of C relative to A is known. In other words, the only unknown quantity in the expression $T = 0$ is the height of C relative to A. The problem thus reduces to finding a height for C that causes T to vanish. A way of doing this is described in Chapter III. Chapter IV discusses methods for determining an initial

---

[2] An "interstation velocity" is the component of the relative geostrophic velocity normal to a vertical plane passing through two adjacent stations.

slope, in this case the slope along AB.

Four-sided cells are treated similarly, except that the slopes along two adjacent sides (rather than just one side) must be given initially. The remaining two interstation slopes are then adjusted to make T vanish.

To see how the method works with several cells, consider the array of cells shown in Figure 4. Assume that the slope along AB is given, as before, and that the remaining interstation slopes are to be determined. Station A will be used as a reference ($h_A=0$), and the heights of the other stations will be determined relative to A. Since the slope of AB is given, the height of B can be calculated immediately. Next the height of C is calculated, using formulas given in Chapter III. That is, a height is selected for C that causes the net transport into the cell to vanish.

As soon as h_C is known, Cell 2 can be treated. In Cell 2, AC plays the same role as AB in Cell 1: it is the side whose slope is known in advance. Here the problem is to find a height for D that causes the net transport into ACD to vanish. Again, the required height can be calculated from the formulas of Chapter III.

In the same way, the heights of E, F, and G can in turn be determined. When Cell 6 (BHFC) is reached the slopes of BC and CF are known and a height must be calculated for H. Cell 7 is treated like Cell 6. In general, an m-sided cell is entered only

when the heights of $m - 1$ of its stations are known. The height of the mth station can be calculated by means of formulas given in Chapter III. It will seldom be necessary to take m greater than 4.

So far it has been assumed that the hydrographic data at each station extend to the ocean floor. Ordinarily, of course, hydrographic casts stop short of the bottom. As a result, the cells must be shortened so that they reach only to the deepest level at which data are available. It will be assumed here that vertical motion at this level is negligible. If this is done each cell is, in effect, closed at the bottom, and the conservation of mass argument still can be used. This is equivalent to assuming that the deep flow, beneath the cell, is divergenceless.

III. TRANSPORT EQUATIONS

Consider an m-sided prism and assume that the heights of all but one of the m stations at the cell's vertices are known. The task is to write an expression for the height of the remaining station. In this context, as above, "height" means height relative to some fixed, level (equigeopotential) reference plane.

We will use a coordinate system in which the xy plane is horizontal and z is measured positive upward. The x axis is directed eastward and the y axis northward. $z = z_b$ at the bottom of the cell, and $z = h$ at the sea surface. The origin of the z axis will be chosen so that $h = 0$ at some one of the stations of the network; then $h \ll z_b$ always.

Using the notation and assumptions of Chapter II, the net mass transport into the cell is

$$T = \oint_S \int_{z_b}^{h} \rho v_n \, dz \, dS$$

$$= \oint_S \int_0^{p_b} \frac{v_n}{g} \, dp \, dS$$

Here p_b is the pressure at the bottom of the cell, and the line integral is taken clockwise around the cell. Let $\partial\tilde{p}/\partial S$ be the baroclinic portion of the pressure gradient. From Equations 2 and 3,

$$v_n = \frac{1}{\rho f}\left(-\frac{\partial \tilde{p}}{\partial S} - \rho_o g \frac{\partial h}{\partial S} + \frac{\partial \tau_s}{\partial z}\right)$$

so that

$$T = \oint_S \int_0^{p_b} \frac{1}{\rho f g}\left(-\frac{\partial \tilde{p}}{\partial S} - \rho_o g \frac{\partial h}{\partial S} + \frac{\partial \tau_s}{\partial z}\right) dp dS$$

$$= -\oint_S \int_0^{p_b} \frac{1}{\rho f g} \frac{\partial \tilde{p}}{\partial S} dp dS - \oint \int_0^{p_b} \frac{\rho_o}{\rho f} dp dS$$

$$-\oint_S \int_0^{p_b} \frac{1}{f} \frac{\partial \tau_s}{\partial p} dp dS$$

$$\equiv T_{bc} + T_{bt} + T_e \qquad (4)$$

T_{bc} and T_{bt} are, respectively, the baroclinic and barotropic transports, and T_e is the Ekman transport caused by wind stress at the sea surface. (It will be assumed that $\tau = 0$ at the bottom of the cell.)

To calculate T_{bc}, note that

$$\left.\frac{\partial \tilde{p}}{\partial S}\right|_{z=\text{const.}} = -\rho \left.\frac{\partial D}{\partial S}\right|_{p=\text{const.}}$$

where $D(z) = g(h-z)$ is the dynamic depth at the point where $\partial \tilde{p}/\partial S$ is being evaluated. Then

$$T_{bc} = \oint_S \int_0^{p_b} \frac{1}{fg}\left(\frac{\partial D}{\partial S}\right)_p dp dS$$

$$= \frac{1}{g}\int_0^{p_b}\left[\oint_S \frac{1}{f}\left(\frac{\partial D}{\partial S}\right)_p dS\right] dp$$

The line integral can be divided into m parts, corresponding to the m sides of the cell. Let f_i be the average value of f along the ith side, and let

$$\oint_S = \sum_{i=1}^{m} \int_i$$

Then

$$T_{bc} \doteq \frac{1}{g} \int_0^{p_b} \left[\sum_{i=1}^{m} \frac{1}{f_i} \int_i \left(\frac{\partial D}{\partial S}\right)_p dS \right] dp$$

$$= \frac{1}{g} \int_0^{p_b} \sum_{i=1}^{m} \frac{D_{2i} - D_{1i}}{f_i} \, dp$$

where D_{1i} and D_{2i} are the dynamic depths shown in Figure 5. In practice D is computed from hydrocast data and is known only at specified standard depths. Using the values at these depths (designated by the superscript j) we can approximate the pressure integral with a finite sum. Thus

$$T_{bc} \doteq \frac{1}{g} \sum_{j} \sum_{i=1}^{m} \frac{1}{2f_i} \left(D^j_{2i} - D^j_{1i} + D^{j+1}_{2i} - D^{j+1}_{1i}\right) \left(p^{j+1} - p^j\right) \qquad (5)$$

The barotropic transport is

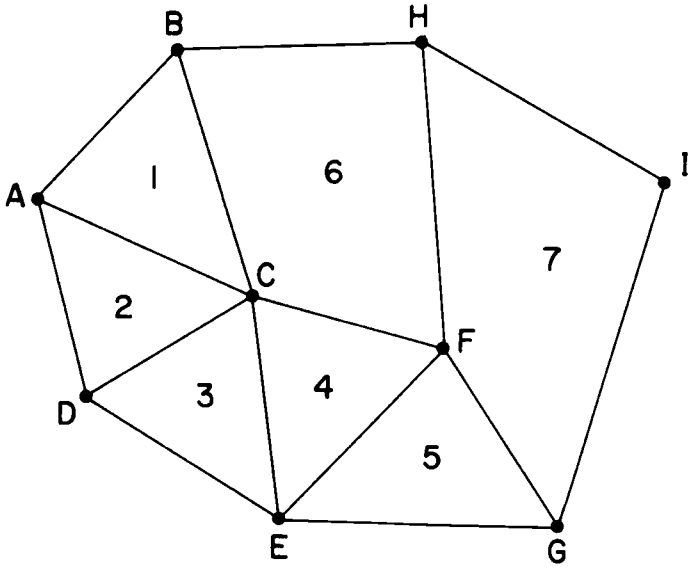

Figure 4. A network of hydrographic stations. If the slope along AB is given, the remaining interstation slopes can be calculated.

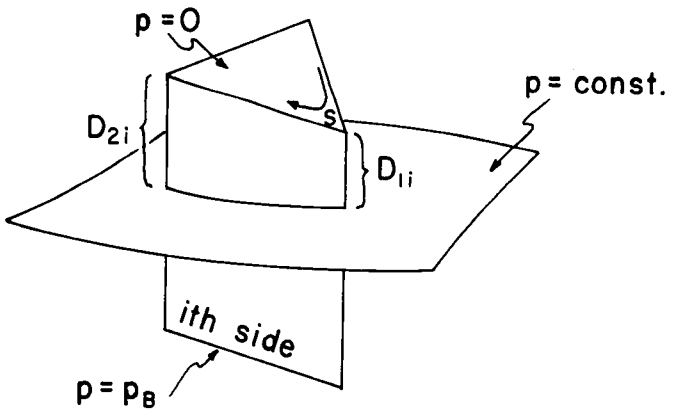

Figure 5. Intersection of an isobaric surface with a 3-sided cell.

$$T_{bt} = - \oint_S \int_0^{p_b} \frac{\rho_o}{\rho f} \frac{\partial h}{\partial S} \, dp dS$$

$$= - \int_0^{p_b} \oint_S \frac{\rho_o}{\rho f} \frac{\partial h}{\partial S} \, dS dp$$

$$= - \int_0^{p_b} \sum_{i=1}^{m} \frac{1}{f_i} \int_i \frac{\partial h}{\partial S} \, dS dp$$

$$= - \int_0^{p_b} \sum_{i=1}^{m} \frac{\Delta h_i}{f_i} \, dp$$

$$= - p_b \sum_{i=1}^{m} \frac{\Delta h_i}{f_i} \qquad (6)$$

The quantity Δh_i is the change in h along the ith side of the cell (proceding clockwise, as in Figure 5).

Finally, the wind-coupled mass transport into the cell is

$$T_e = - \oint_S \frac{1}{f} \int_0^{p_b} \frac{\partial \tau_s}{\partial p} \, dp dS$$

$$= - \oint_S \frac{1}{f} [\tau_s(p_b) - \tau_s(0)] dS$$

$$\doteq \oint_S \frac{\tau_s(0)}{f} \, dS$$

if it is assumed that the vertical shear is negligible at the bottom of

the cell. Let τ_i be the average value of $\tau_s(0)$ along the ith side of the cell, and let L_i be the length of the ith side. Then approximately

$$T_e = \sum_{i=1}^{m} \frac{\tau_i L_i}{f_i} \tag{7}$$

The net mass transport into the cell vanishes. Thus

$$T_{bc} + T_{bt} + T_e = 0$$

or, substitutiing from Equation 6,

$$p_b \sum_{i=1}^{m} \frac{\Delta h_i}{f_i} = T_{bc} + T_e \tag{8}$$

Now suppose that the sides of the cell are numbered so that i equals 1 and 2 on the two adjacent sides whose slopes are not known. Then $\Delta h_3, \Delta h_4, \ldots, \Delta h_m$ are known quantities, but Δh_1 and Δh_2 are not. Equation 8 can be written

$$\frac{\Delta h_1}{f_1} + \frac{\Delta h_2}{f_2} = - \sum_{i=3}^{m} \frac{\Delta h_i}{f_i} + \frac{T_{bc} + T_e}{p_b} \tag{9}$$

and we also have

$$\Delta h_1 + \Delta h_2 = - \sum_{i=3}^{m} \Delta h_i \qquad (10)$$

A simultaneous solution of Equations 9 and 10 yields

$$\Delta h_2 = \frac{\sum_{3}^{m} \Delta h_i \left(\frac{1}{f_i} - \frac{1}{f_1}\right) - \frac{1}{p_b}(T_{bc} + T_e)}{\frac{1}{f_1} - \frac{1}{f_2}} \qquad (11)$$

Then

$$\Delta h_1 = - \sum_{i=2}^{m} \Delta h_i$$

Since all the quantities on the right-hand side of Equation 11 are given or can be calculated from given information, Equation 11 is the desired solution. Whenever the heights of $m-1$ stations of an m-sided cell are known, the height of the remaining station can be found from Equation 11. For example, if the heights of Stations A and B of Figure 3 are known and that of Station C is not, and $i = 2$ on BC, then $h_C = h_B + \Delta h_2$, where Δh_2 is given by Equation 11.

IV. STARTING METHODS

The solution outlined above requires hydrographic and wind data. In addition, to get started, we need the slope of the sea surface between two adjacent stations. There are several ways of obtaining this slope. It may, for example, be possible to utilize direct measurements of the surface current between a pair of stations.

Failing this or other means, hydrographic and wind data will yield a starting slope. To see how, return to Figure 3 and suppose that the cell shown there contains a level of no horizontal motion.[3] Suppose also that the cell is small in area, so that the depth of no motion is nearly the same on all three sides. The first step is to calculate the net Ekman transport into the cell, using Equation 7. Next, an arbitrary reference depth $z = z_{ref}$ is selected, and the net geostrophic transport into the cell $(T_{bc} + T_{bt})$ is calculated, assuming that z_{ref} is the depth of no motion.[4] Finally, the geostrophic transport and the Ekman transport are compared. If z_{ref}

---

[3] Stommel (1956) has pointed out that the depth of no meridional flow need not be the same as the depth of no zonal flow. It will be assumed here, however, that the two depths are the same, or at least are close together, so that minimal error is introduced by assuming that a level of no horizontal motion exists.

[4] To do this, compute the speeds $\tilde{v}_n(z) = -(\partial\tilde{p}(z)/\partial s)/\rho(z)f$ at all depths and on all three sides of the cell, subtract $\tilde{v}_n(z_{ref})$, multiply by $\rho(z)$, and integrate over the entire vertical portion of the cell. ($\tilde{v}_n$ is the horizontal velocity normal to the vertical cell boundary, and relative to the sea surface. That is, $\tilde{v}_n(h) = 0.$)

is the depth of no motion, the two transports will be equal in magnitude but opposite in sign; otherwise they will be unequal. The procedure is systematically to select and test different reference depths until the level of no horizontal motion is encountered. This is essentially a trial-and-error technique. Once the level of no motion is known the slopes along AB, BC and CA can be found from the hydrographic data. Note that this technique provides not just one intersection slope, but three (or m, if the starting cell has m sides).

This starting method is quite general, in the sense that it can be used anywhere in the ocean. In his analysis of the Peru Current, Wyrtki used a specialized version suited for coastal waters. His approach is illustrated in Figure 6a. Here the network of hydrographic stations is bordered on one side by a coastline. Each of the three cells adjacent to the coast (the cells numbered 1, 2, and 3) is a starting cell, and the technique just described is applied to each in turn.[5] If Stations A, D, F, and H are sufficiently close to shore, one can assume that no water flows through ADFH at any depth. As soon as the interstation sea surface slopes for these cells are known, the

[5] Wyrtki did not actually use the trial-and-error procedure discussed above. Instead, to find the depth of no motion in a starting cell, he used a method of successive approximations. The trial-and-error technique has been emphasized here because it is conceptually simpler, and is the method used by the computer program described in the next section.

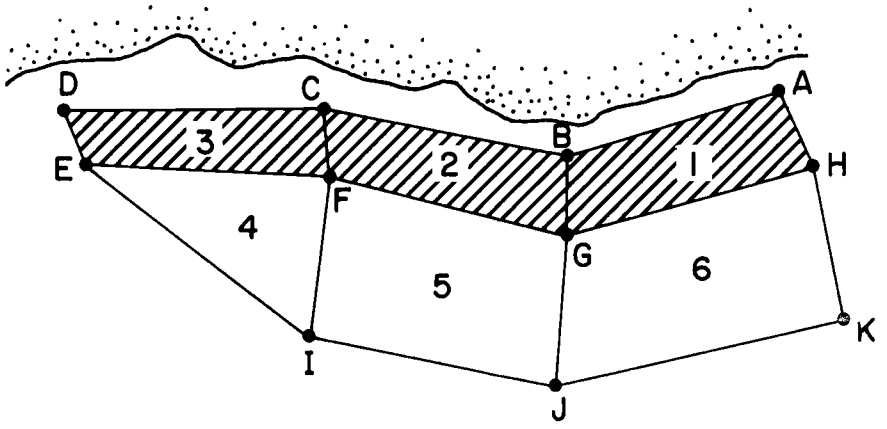

Figure 6a. Wyrtki's starting method for a network of stations adjacent to a coastline. Cells 1, 2, and 3 are starting cells.

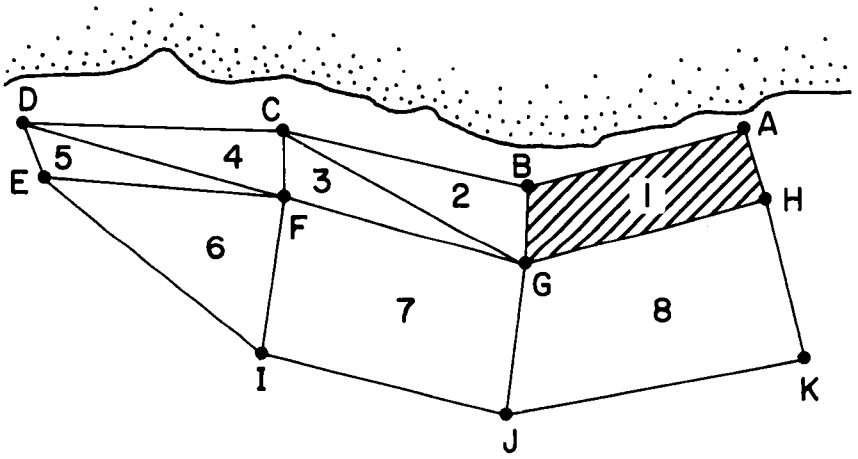

Figure 6b. An alternative solution for a network of stations adjacent to a coastline. Cell 1 is a starting cell.

station heights relative to the reference station (Station A, say) can be determined. This starting method produces a continuous line of stations parallel to the coast (BCEG in Figure 6a) whose heights are known. These constitute a base line for extending the analysis farther offshore. Given this base line, the heights of I, J, and K can easily be found by applying the formulas of Chapter III to cells 4, 5, and 6 in turn.

It should be pointed out, however, that Wyrtki's starting method is not the only starting method appropriate for a coastal network. Figure 6b shows the same network handled in a different way. In Figure 6b there is only one starting cell, Cell 1; the others are cells of the type described in Chapter III. There is, as it happens, a distinct disadvantage to a solution that requires several starting cells. It is necessary to assume the existence of a level of no horizontal flow in a starting cell. As Stommel has shown (1956), this is a risky assumption. Accordingly, a solution that uses just one starting cell may be more reliable than one that uses several.

The cells just described, in which a level of no horizontal motion is found by trial-and-error or by some other method, will be called, variously, starting cells, turning cells, or Type I cells. All other cells (these were described in Chapters II and III) will be called Type II cells.

V. COMPUTER PROGRAM

A computer program has been prepared that performs the calculations described above. Using hydrographic and wind data, it computes the height of every station in a specified network relative to a selected reference station. In addition, the program prints out a useful sequence of absolute geostrophic current speeds and transports, and the interstation Ekman transports.

A simplified flow diagram of the program is shown in Figure 7. The program consists of a control section and three subroutines. The control section is named CNTROL and the subroutine names are PRISM1, PRISM2, and TRANSP. PRISM1 computes the station heights in a Type I cell, and PRISM2 computes the heights in a Type II cell. TRANSP computes and prints out the interstation geostrophic mass transports.

The program steps through the network cell by cell, calling the appropriate subroutine each time a new cell is entered. The cells are numbered 1 through N by the program user. The calculations begin with Cell 1 and end with Cell N. Thus, Cell 1 is ordinarily a tuning cell, and the cells must be ordered in such a way that when a given Type II cell is reached, only one of its station heights remains to be determined.

Direction is provided by an <u>itinerary</u> which consists of a series

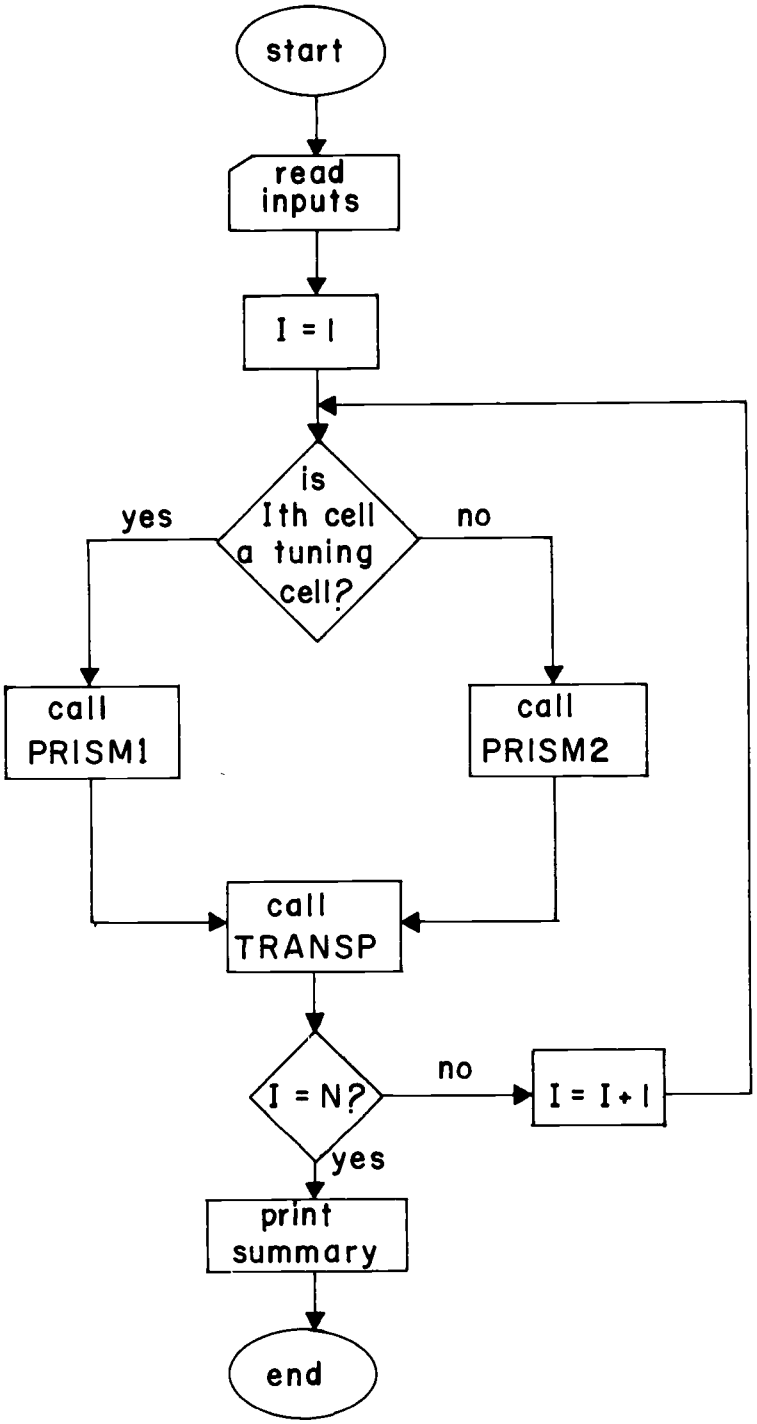

Figure 7. Simplified flow diagram of the computer program.

of input cards, one for each cell. Each station in the network is given an identification number. The itinerary card for a given cell contains the ID numbers of the stations in the cell, and a code that tells how many sides the cell has, whether it is a Type I or Type II cell, how deep it is, and so forth. In the case of a Type II cell, the order of the ID numbers indicates which station is the "new" station whose height is to be determined.

Different starting methods are allowed. If the heights of two adjacent stations are known from previous considerations, these heights can be input and the analysis can proceed without benefit of tuning cells. If tuning cells are used they may be located in deep water, or along the shore as in Figure 6. The program user may specify a single tuning cell or many. If a series of tuning cells along a coast is used, as in Figure 6, the program will automatically adjust the inter-station slopes between adjacent tuning cells so that they agree.

Cells may have either three or four sides, and the program user can seal off one side of any type of cell. When this is done there is no flow, at any depth, through that side. This option is appropriate in cases where a cell abuts a coastline; its use is equivalent to imposing a boundary condition of no flow through the coast.

Pressure, rather than geometric depth, is the independent variable in the vertical direction. The pressures p^j of Equation 5 are input to the program as data. Any sequence of p^j values is permitted, but the same sequence is used at every station of the network.

That is, one sequence is input and is used throughout the network. Also input are the dynamic depths, at each station, of the specified pressure surfaces. Each cell extends from the ocean surface to a depth at which the pressure is equal to p_b, where p_b is a selected p^j value. Different values of p_b can be specified for different cells.

Additional inputs are the latitude and longitude of each station in the network, and the direction and magnitude of the wind stress at each station.

To find the level of no motion in a tuning cell, the program initiates a trail-and-error search. First, it selects the surface $p = p_b$ as a reference surface and computes the net transport into the cell assuming that $v(p_b) = 0$. If this transport does not vanish, the program moves upward to the next higher pressure surface[6] and repeats the procedure. If the new level also is not a zero surface, the program checks to see if the sign of the transport has changed. If it has, the zero surface lies somewhere between $p = p_b$ and the next higher (shallower) pressure level, and a linear interpolation is made to find its exact depth. Failing a change in sign, the program moves upward again, to the next pressure level, and checks again for a null transport or a change in sign. This continues until the level of no

---

[6] The surface defined by $p = p^r$, where r is given by $p_b = p^{r+1}$.

motion is located or the sea surface is reached. In the latter case execution is terminated. Failure implies that the level of no meridional motion and the level of no zonal motion lie either at significantly different depths or outisde the range $0 \leq p \leq p_b$.

Results are printed out cell by cell. The printout for each cell includes

1. The dynamic height of each station in the cell.
2. A table of interstation geostrophic current speeds relative to the sea surface. (Speeds are printed out for each side of the cell and for each input pressure surface.)
3. A table of absolute interstation geostrophic current speeds.
4. The Ekman mass transport through each side of the cell.
5. A table of absolute interstation geostrophic mass transports.

A listing of the program and a description of the input format are included here as an appendix.

VI. ARABIAN SEA ANALYSIS

During late June and early July of 1963 the Royal Research Ship Discovery occupied a series of stations in coastal waters south of the Arabian peninsula. Hydrographic data procured during this cruise were used as inputs for an analysis of the type discussed above in Chapters II, III and IV. The calculations were performed by the computer program of Chapter V.

As a first step, the region shown in Figure 1 was divided into a number of polygonal cells. These are shown in Figure 8. The numbers in the cells indicate the order in which they were taken up by the computer program. Cell 1 is a Type I cell; all others are of Type II. Table 1 shows the depth of the bottom of each cell, and the water depth under each cell. The shoreward boundary of the array was, in effect, sealed: it was assumed that no water passed through the coastal sides of Cells 23 through 26--that the flow at this distance from shore was parallel to the coastline at all depths. This assumption and some alternatives will be examined below.

Wind data were available for each station. Wind stresses at the sea surface were computed from

$$\vec{\tau} = \rho_{air} C_d W \vec{W} \tag{12}$$

using $\rho_{air} = 1.2 \times 10^{-3}$ gm/cm^3 and $C_d = 2.6 \times 10^{-3}$. W is

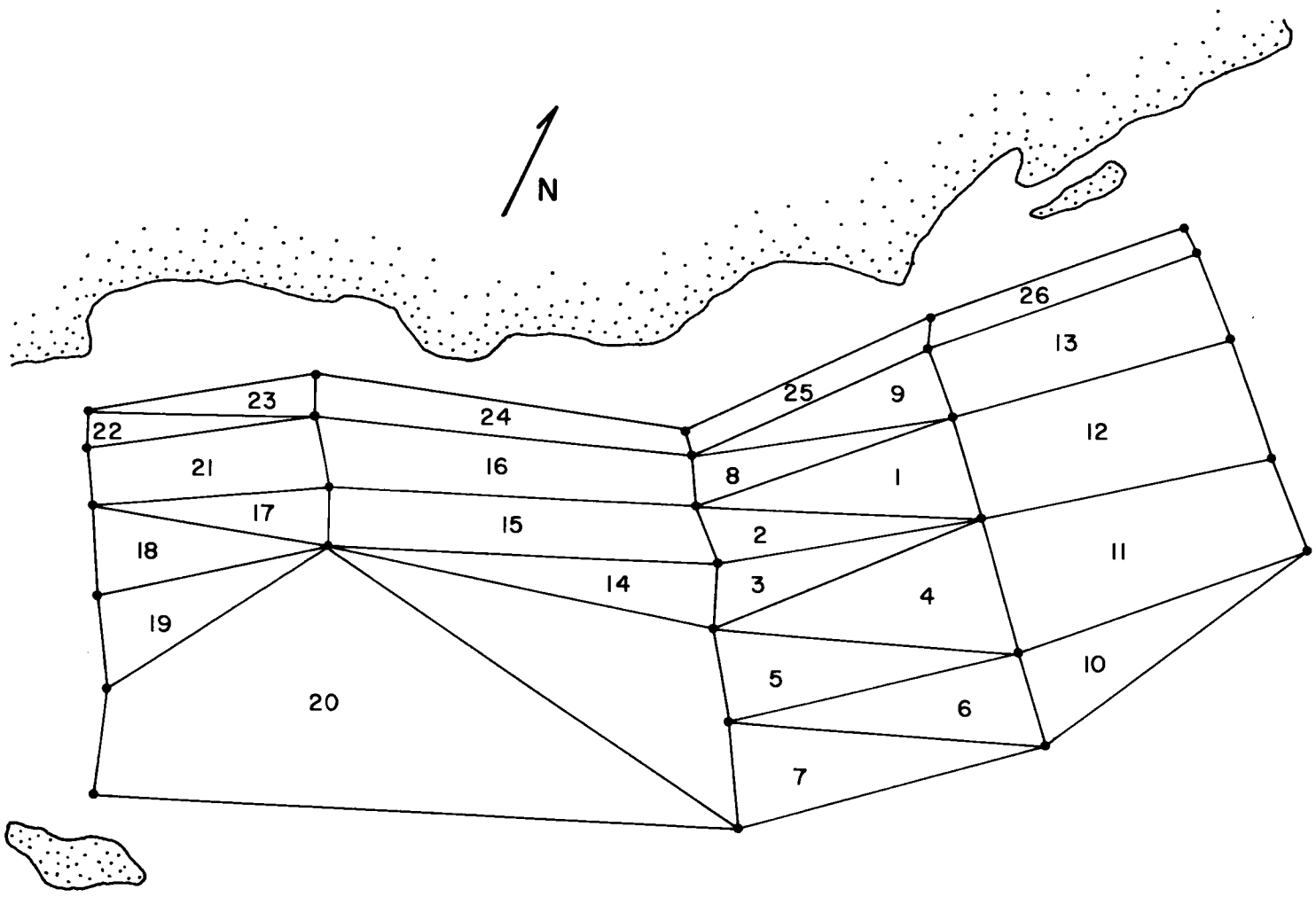

Figure 8. Network of cells. Cell 1 is a Type I cell; the rest are Type II.

Table 1. Cell depths and water depths.

Cell	Pressure at bottom of cell (p_b)	Water depth
1	3000 db	3300-3900 m
2	3000	3600-4000
3	3000	3600-4000
4	3000	3600-3900
5	3000	3700-4000
6	3000	4000
7	3000	3800-4000
8	3000	3200-4000
9	3000	3200-3600
10	3000	3600-4000
11	3000	3600-3900
12	3000	3300-3600
13	3000	3200-3500
14	2000	3000-4000
15	2000	2900-4000
16	2000	2600-3800
17	2000	2000-3000
18	2000	2000-3000
19	2000	2600-3000
20	2000	2700-3800
21	2000	2000-2900
22	1600	2200-2600
23	1600	2200-2600
24	900	1200-2600
25	900	1100-3200
26	1000	1100-3300

windspeed in cm/sec. The stresses used in the transport calculations were smoothed values, obtained as follows. First, all of the wind vectors recorded in the scientific log of the expedition were converted into stresses, by means of Equation 12. Second, the ocean was divided into one-degree squares, and the stresses in each square were averaged. Third, each station was assigned the averaged stress of the square containing it. Fourth, the magnitudes and directions of the averaged stresses were plotted as functions of distance offshore, separately for each line of stations. Fifth, smooth curves were passed through the resulting plots.[7] The magnitude and direction of the final, smoothed wind stress for each station were then read off the appropriate curves.[8] The smoothed values are given in Table 2. This smoothing procedure was selected after several other methods had been tried, all of which either obscured important trends in the wind data, or led to unreasonable transports. It should be mentioned that the geostrophic transports calculated from Equation 8 are quite sensitive to $\text{curl}_z \vec{\tau}$, so that an accurate wind input is necessary. The general wind picture revealed in Table 2 agrees well with that given by Ramage (1965) for this area.

---

[7] In many cases the plots were roughly linear and least-squares lines of best fit were used.

[8] Smoothed stresses greater than 6 dynes/cm^2 were reduced to 6 dynes/cm^2. This was done because Equation 12 appears to overestimate τ for large windspeeds.

Table 2. Smoothed wind stresses. τ is the magnitude of the stress, and θ is the compass direction toward which the wind was blowing.

Station		τ (dynes/cm^2)	θ (degrees)	Station		τ (dynes/cm^2)	θ (degrees)
5008	line 1	1.6	10	5049	line 4	5.1	40
5009		2.0	10	5050		5.2	40
5011		2.8	10	5052		5.3	40
5014		4.5	10	5054		5.8	40
5015		4.6	20	5056		6.0	40
5017		4.7	30	5057		6.0	40
5026	line 2	3.0	35	5063	line 5	2.8	30
2057		3.3	35	5065		3.0	30
5029		3.7	30	5067		3.3	30
5031		4.4	30	5069		4.0	30
5037	line 3	4.4	40	5070		4.5	30
5038		4.6	40				
5040		5.2	40				
5042		5.7	40				
5044		6.0	40				
5045		6.0	40				
5046		6.0	40				

Figures 9 through 13 show some of the results of the analysis. Figure 9 is a plot of the absolute dynamic topography of the sea surface. It can be compared to Figure 10, which shows the dynamic topography relative to the 1000 db surface. The differences between the two are not great except in the region north of Socotra, where the flow is somewhat weaker in Figure 9.[9] The most interesting features of Figure 9 are three large eddies in the geostrophic current. The westernmost eddy appears to be permanent, since it has also been found during the winter monsoon, shifted slightly northward (Seryi and Khimitsa, 1963).

Figures 11, 12, and 13 show the mass transports in the region studied. Figure 11 gives transports between the surface and 100 db. Figure 12 shows those between 100 db and 300 db, and Figure 13 gives those between 300 db and 700 db. The transports were computed under the assumption that the Ekman flow is confined to the upper 100 m.

The dominant flow in the upper layer (0 to 100 db) is northeastward with a superimposed offshore component caused by the wind. The offshore transport is balanced by water upwelled throughout the region. Upwelling is most intense in a narrow band along the coast. Seaward of this is a narrow strip in which the vertical motion is weak

---

[9] That the analysis technique smooths rather than exaggerates the topography relative to 1000 db is encouraging. If the technique were invalid, one would expect the results to show signs of "blowing up."

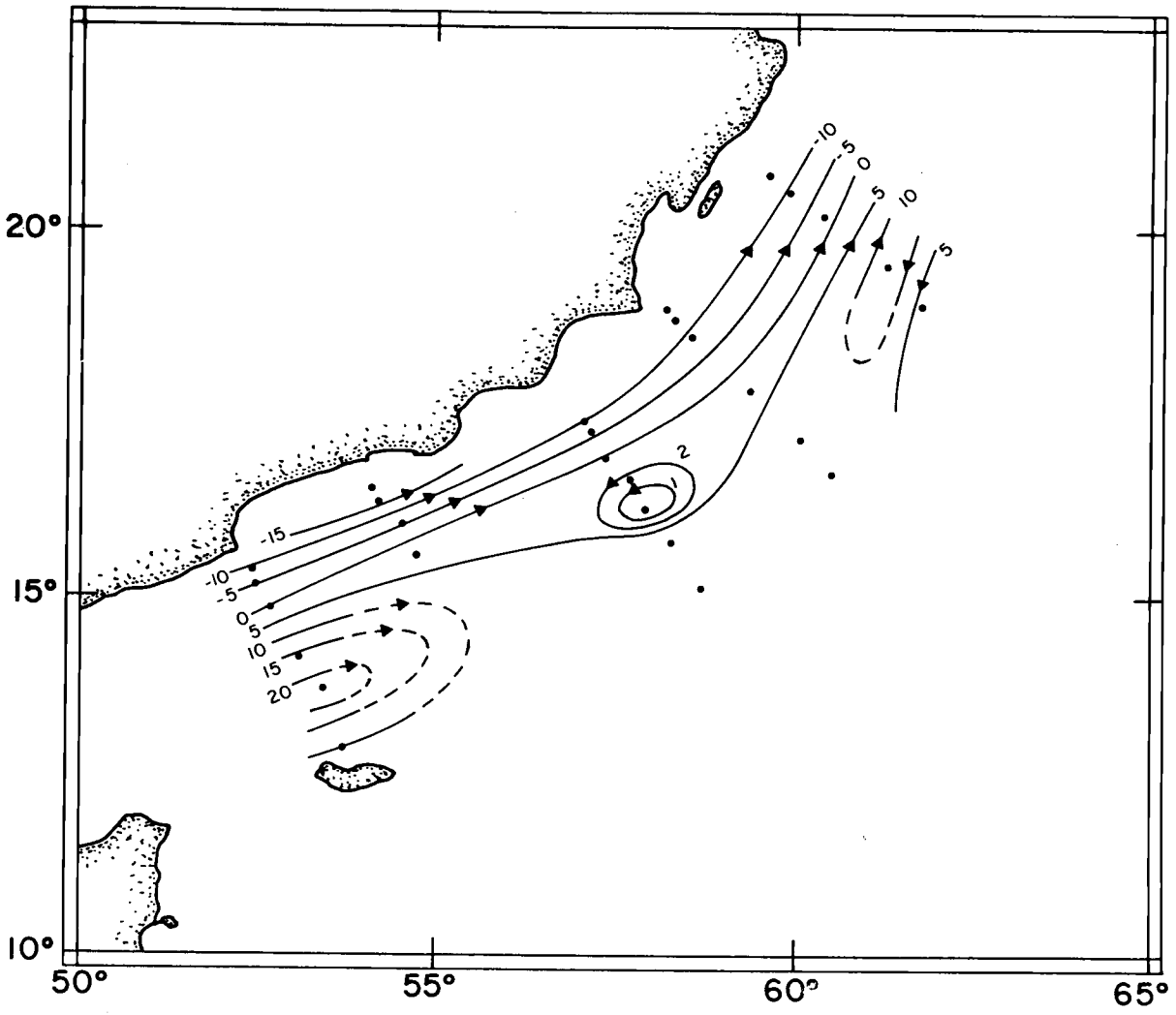

Figure 9. Absolute dynamic topography of the sea surface. h = 0 at Station 5040. (Units: dynamic cm).

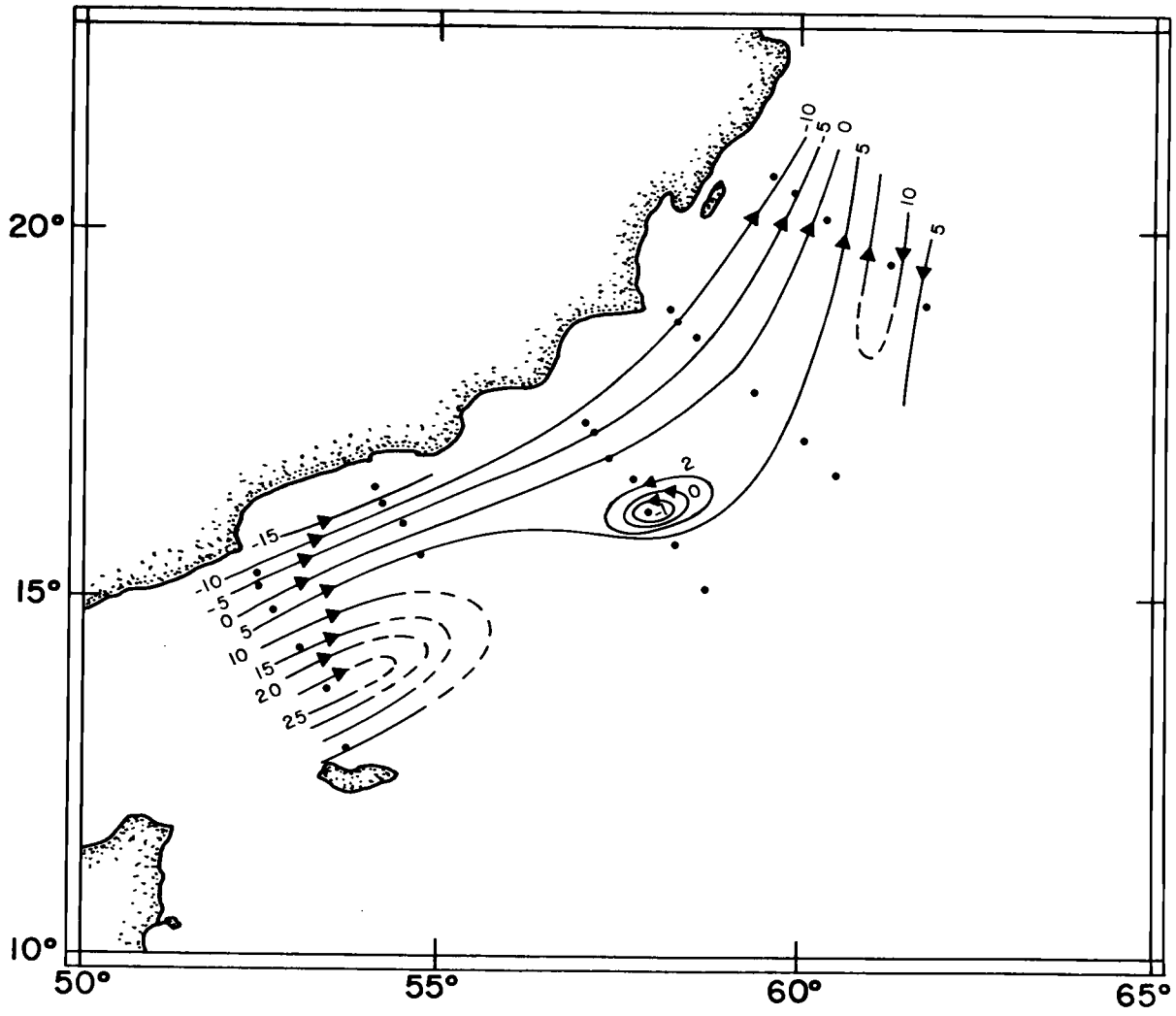

Figure 10. Dynamic topography of the sea surface relative to 1000 db. h = 0 at Station 5040. (Units: dynamic cm).

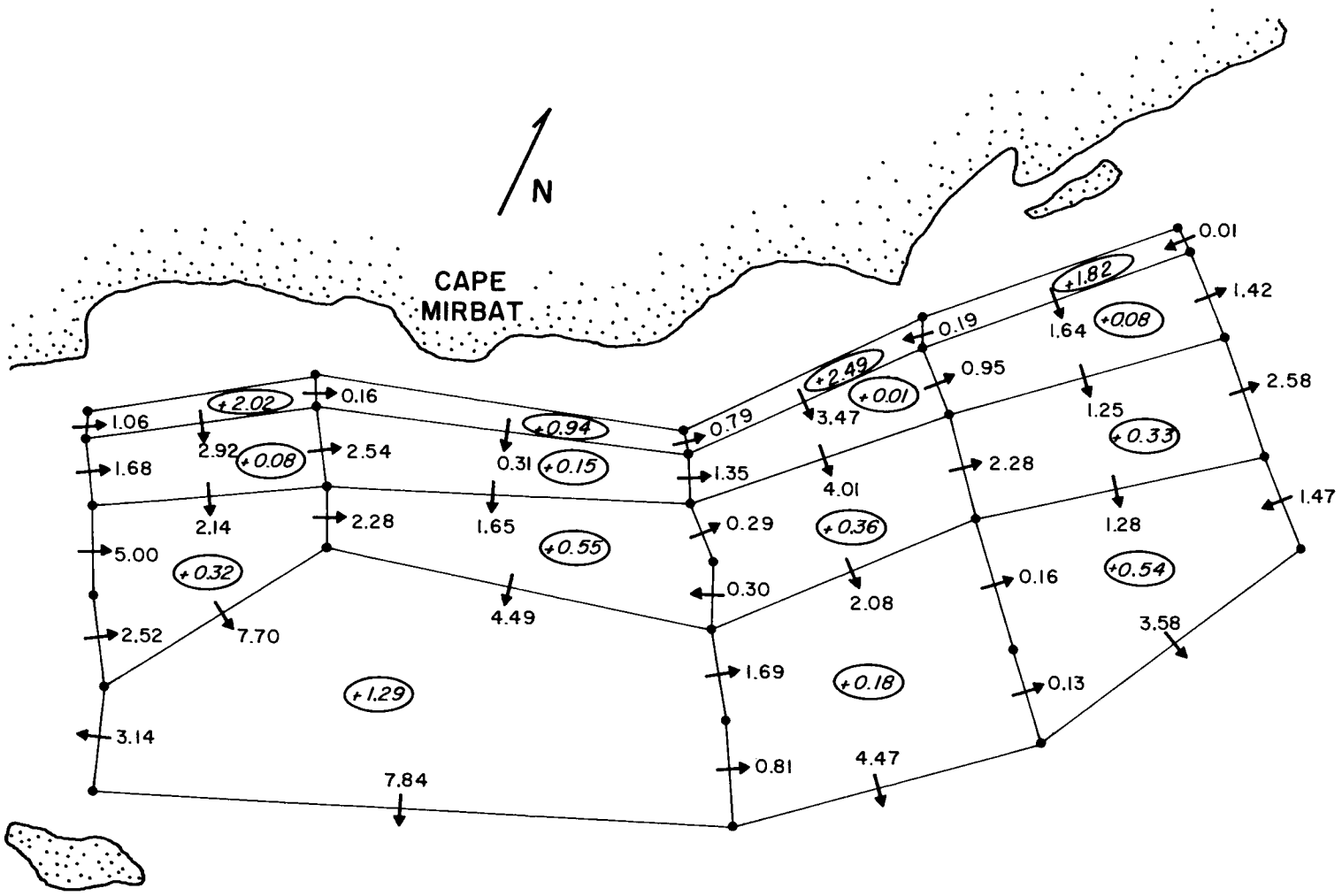

Figure 11. Horizontal mass transports between the ocean surface and 100 m. The circled numbers are vertical mass transports at 100 m. (Units: 10^6 tons/sec).

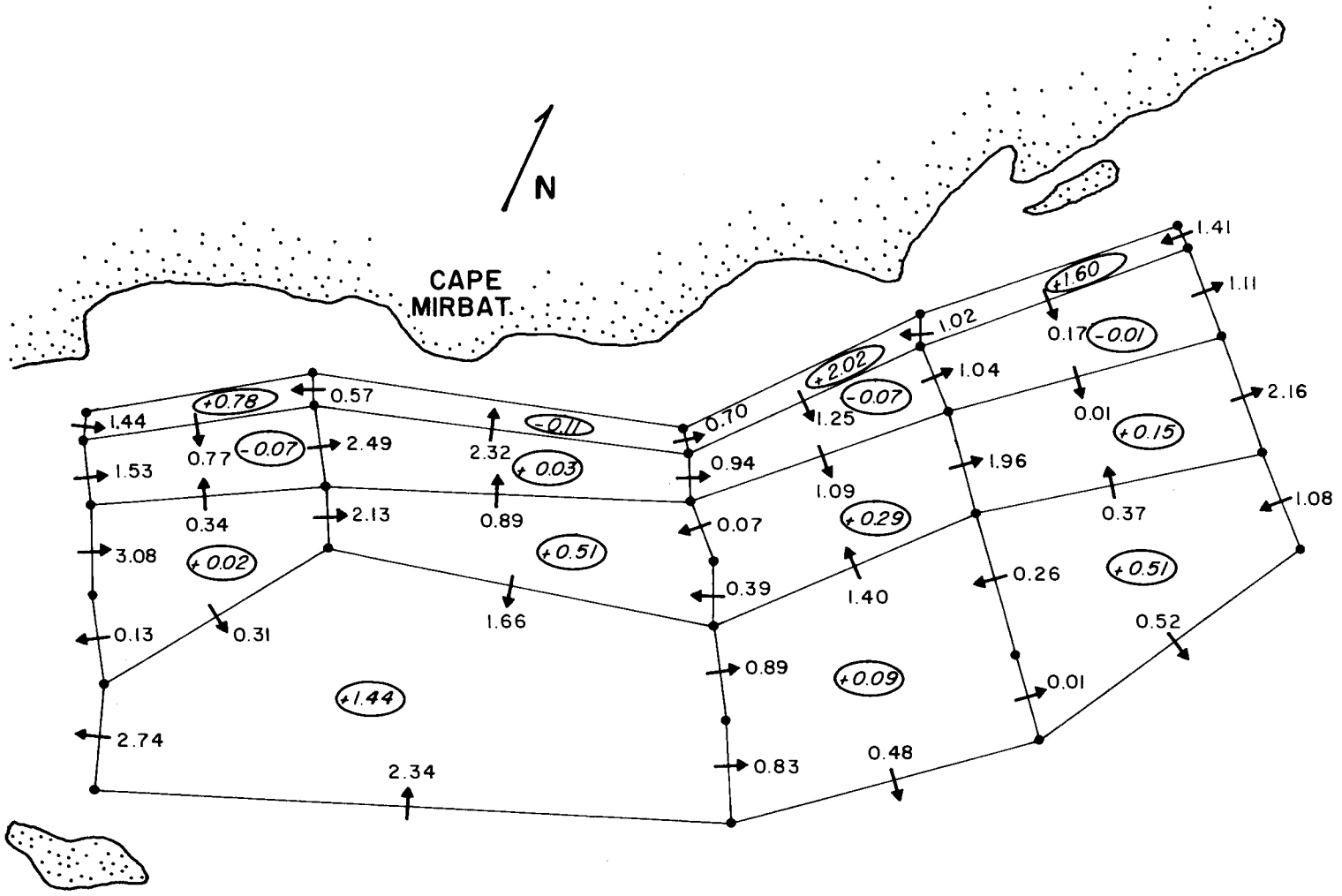

Figure 12. Horizontal mass transports between 100 m and 300 m. The circled numbers are vertical mass transports at 300 m. (Units: 10^6 tons/sec).

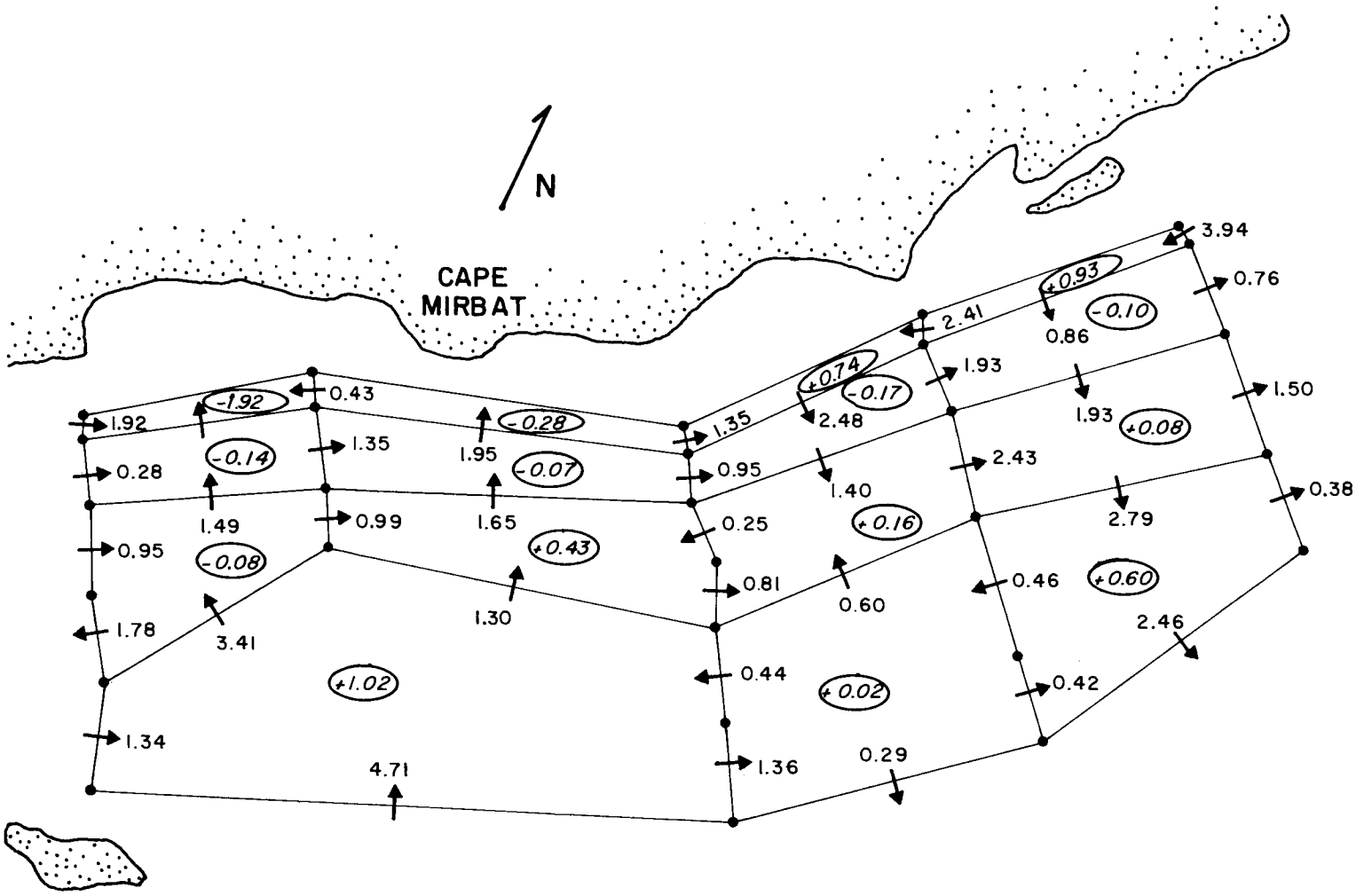

Figure 13. Horizontal mass transports between 300 m and 700 m. The circled numbers are vertical mass transports at 700 m. (Units: 10^6 tons/sec).

and mostly upward at 100 m, and mostly downward below 100 m. Farther offshore, paralleling the coast, is a second, broader, less intense upwelling area. The vertical speeds at 100 m are on the order of 10^{-2} cm/sec in the inner upwelling band, and 10^{-3} cm/sec in the outer band.

Much of the upwelled water is supplied by inshore and longshore flow at comparatively deep levels, as indicated by appreciable upward speeds at 300 m and 700 m in many of the cells. This deep supply contrasts with that observed elsewhere in upwelling areas. Wyrtki (1963) showed that upwelling in the Peru Current is confined to the upper 100 m. Sverdrup and Fleming (1941) found that upwelling in the California Current probably occurs only in the upper 200 m. Smith, Patullo, and Lane (1966) showed that upwelling off the Oregon coast takes place in the upper 150 m.

The intermediate transports shown in Figures 12 and 13 are confused and irregular. This may indicate that the flow below 100 m is dominated by large-scale turbulence. Turbulence of this sort might well play an important role in the lateral transfer of momentum from the Somali Current to the Arabian land mass.

The numbers that appear in Figures 11, 12, and 13 are felt to be most reliable in Cells 1 through 13, and least reliable in Cells 23 through 26. The first 13 cells extend from the ocean surface to a depth of 3000 m. It will be recalled that the analysis technique

assumes that the flow beneath each cell is approximately divergence-less. For cells extending to 3000 m this requirement is probably met. Cells 14 through 21 reach only to 2000 m, however, and for these the assumption may not be as good. Cells 22 through 26, which lie over the continental slope, are even shallower and are suspect for the same reason.

The last four cells, numbers 23 through 26, are further suspect because of the assumption that no water passed through the coastal perimeter of the array. This assumption was motivated by the nearness of the coast; its correctness, however, is open to doubt. Figure 14 shows a series of subsurface current measurements made close to shore during June and July of 1963, using neutrally buoyant floats. The vectors labelled a through f denote measured currents. It can be seen that a, c, d, and f have appreciable onshore-offshore components, contrary to the no-flow assumption. For the sake of comparison, Figure 14 also shows a set of currents calculated from Equations 2 and 3. These are labelled α through ϵ. α is the calculated current closest to a, β is closest to b, and so on. Although the two sets of currents are not close enough together geographically for comparisons to be decisive, the good agreement between e and ϵ, and the partial agreement between a and α, are encouraging.

There are at least two possible alternatives to the no-flow

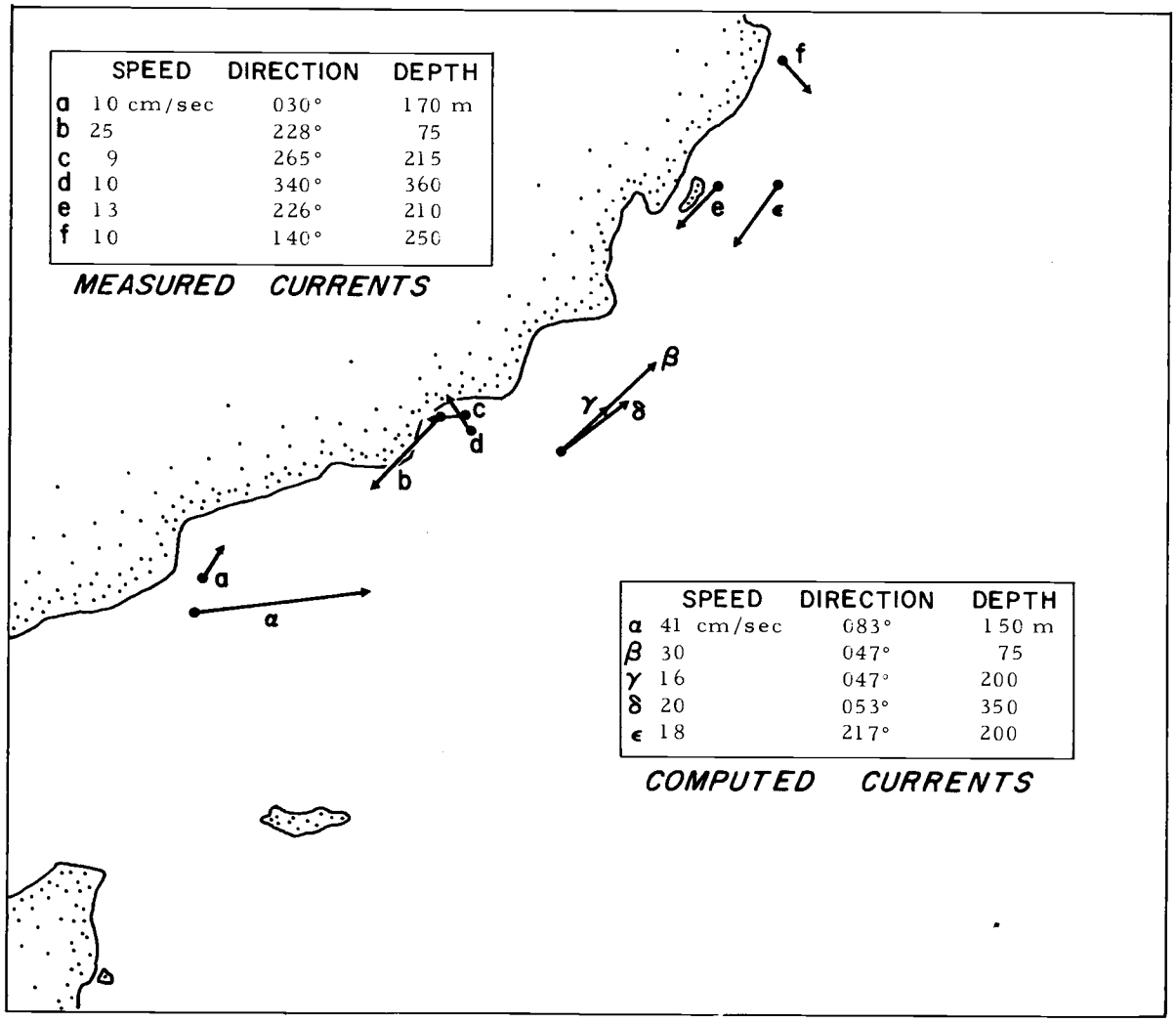

Figure 14. Measured and computed currents close to shore.

assumption: (1) free flow through the coastal boundary, and (2) no net flow through the boundary. The latter possibility is interesting. It might, for example, be reasonable to assume the existence of an unimpeded Ekman transport away from shore through the boundary, balanced by a shoreward geostrophic flow, equal in magnitude, at a deeper level. Adoption of this viewpoint (no net flow) would not affect the computed station heights or any of the horizontal transports shown in the figures; it would change the vertical transports in the four boundary cells.

The other possibility (free flow through the boundary) is less attractive. It seems unlikely that the coastline would not tend to suppress onshore-offshore motion over the continental shelf. In any case, whether the no-flow assumption is correct, partly correct, or wholly incorrect, only the four boundary cells are affected. The computations were arranged so that these cells were done last; none of the results for the other cells depend on the correctness of the treatment of the shoreline cells.

Both the vertical extent of the upwelling shown in Figures 11, 12, and 13, and the large vertical velocities, indicate unusual vigor. The reason for this vigor can probably be found in the strength and steadiness of the monsoon and in the spatial distribution of wind stresses shown in Table 2. Along each line of stations the wind stress increased with distance offshore. This produced, over the entire

region, a divergence in the Ekman flow and a corresponding convergence in the geostrophic flow below 100 m. Thus upwelling was not confined to a narrow strip along the coast, as it would have been if τ had been uniform, but took place throughout the region in which $\text{curl}_z \vec{\tau}$ was positive, an area nearly 1000 km long and at least 400 km wide. Because of the great breadth of the upwelling zone, the upwelled water could not be supplied from within the surface layer. In general, a shallow source is possible only if the region of upwelling is small in at least one horizontal direction. A long, narrow upwelling region, for example, can be supplied by shallow flow toward it, normal to its axis (Figure 15). But if the breadth of a linear upwelling area is greatly increased, then either the supply speed V_s must increase proportionately, or the thickness d of the supply layer must increase. The latter is more likely, and it is probably this or something like it that is responsible for the deep supply indicated in Figures 11, 12 and 13.

Independent evidence of upwelling is shown in Figures 16, 17, and 18, which are taken from the Preliminary Report of the Discovery cruise (The Royal Society, 1963). Figure 16 gives surface temperatures along the Arabian coast, and Figures 17 and 18 show isocontours of temperature and phosphate, respectively, in a vertical section extending from Station 5033 to Station 5046. According to Figure 16, upwelling was most intense near the coast and east of Cape Mirbat.

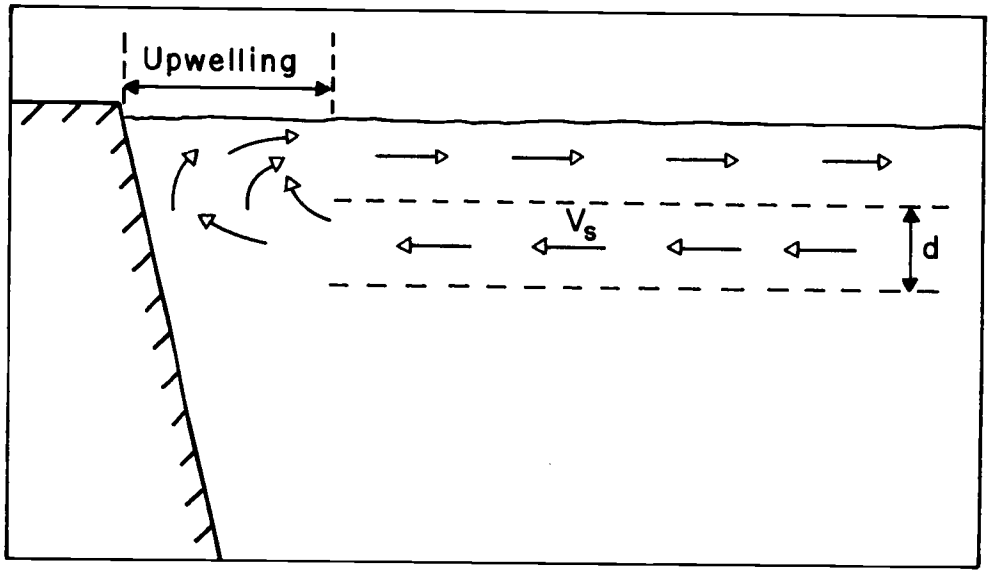

Figure 15. Upwelling along a coast.

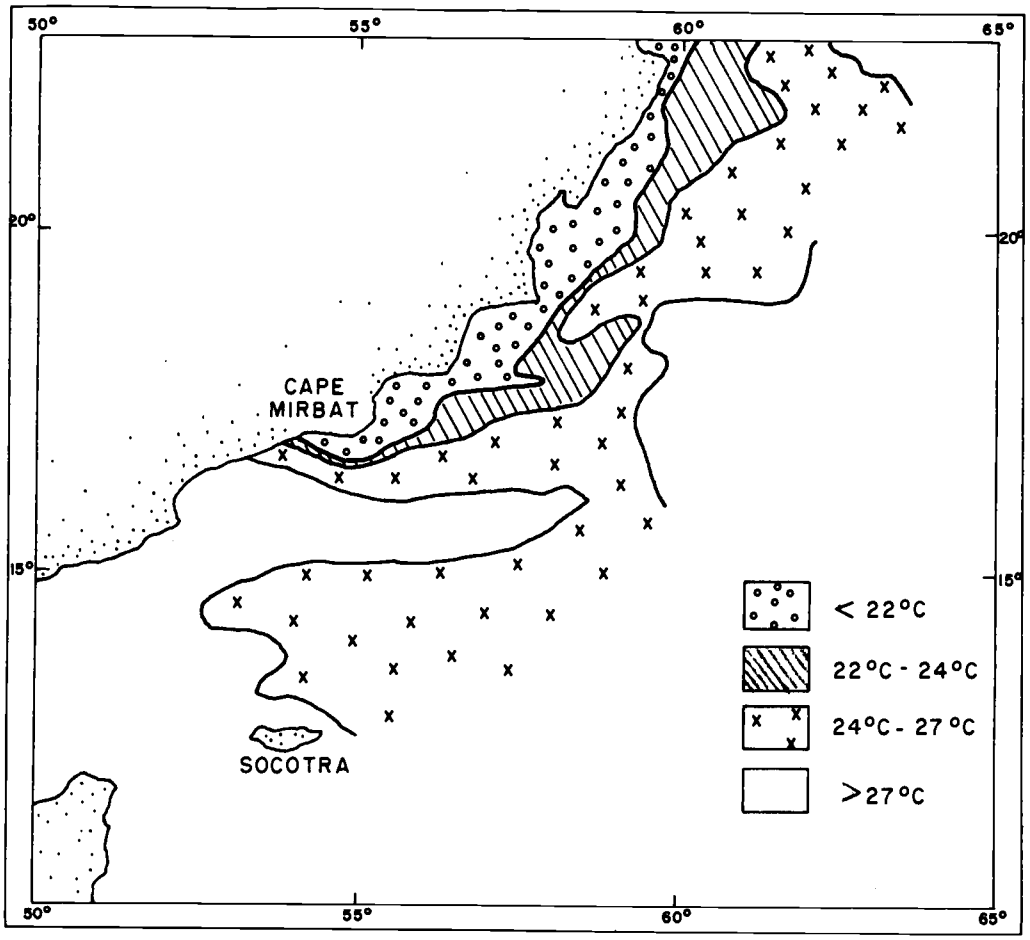

Figure 16. Sea surface temperature, 25 June to 22 July 1963.

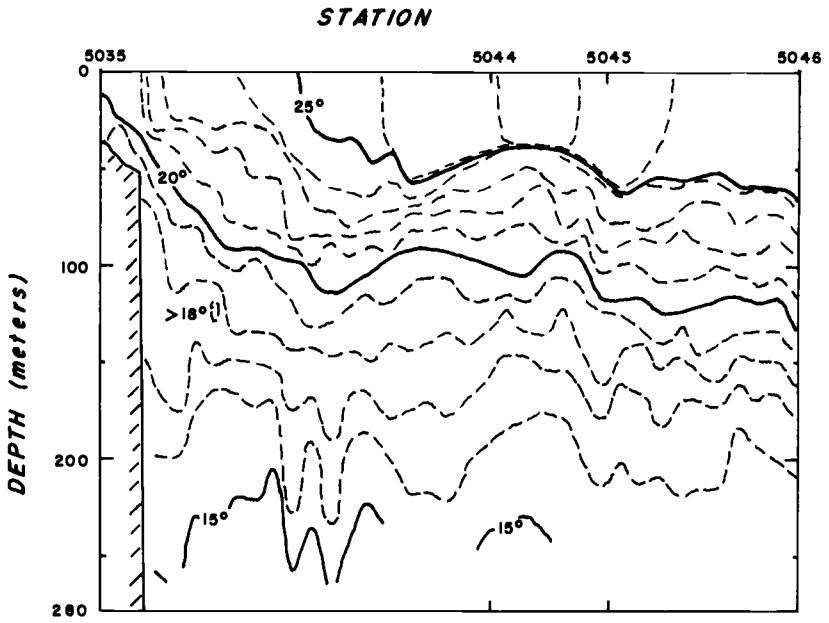

Figure 17. Vertical section showing distribution of temperature from bathythermograph observations on Line 3.

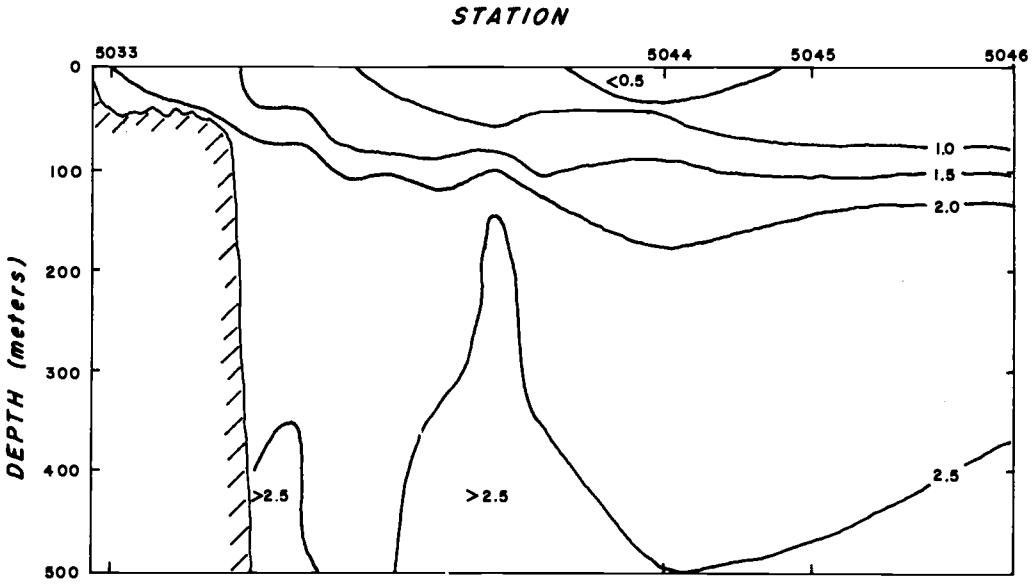

Figure 18. Vertical section showing the distribution of inorganic phosphate (μg ats P/l) on Line 3.

This does not wholly agree with Figure 11, which shows intense upwelling both east and west of Cape Mirbat. It is likely, however, that the effects of upwelling west of the Cape were obscured in Figure 16 by an inflow of warm surface water from the Gulf of Aden.

The sloping contours in the upper parts of Figures 17 and 18 indicate upward motion across the entire section, down to a depth of at least 150 m. The comparatively level temperature contours below 150 m in Figure 17 indicate either that upwelling did not occur below 150 m, or that the vertical velocities, while possibly large, did not vary significantly with distance offshore below 150 m. An interesting detail of Figures 17 and 18 is a pronounced downward bow in the temperature and phosphate contours about 100 km offshore and below 150 m. This coincides nicely with the band of downwelling that extends through Cells 21, 16, 8, 9, and 13 in Figures 12 and 13.

Although the vertical speeds quoted above (10^{-2} cm/sec at 100 m near the coast) are high, they are in agreement with those predicted by Yoshida's theory. Yoshida (cited in Smith, 1967) developed a two-layered coastal upwelling model in which, for τ constant, the vertical velocity at the base of the upper layer is given by

$$w = \frac{k}{\rho f} \tau_p e^{kx} \qquad (13)$$

where $k = f(gh\Delta\rho/\rho)^{-1/2}$ · ρ is the density of the upper layer, $\Delta\rho$

is the density difference between the two layers, h is the thickness of the upper layer, τ_p is the component of $\vec{\tau}$ parallel to the coastline, and x is distance offshore. For Cells 22 and 23 of Figure 8, $\rho \doteq 1.0245$ gm/cm^3 and $\Delta\rho \doteq 0.0025$ gm/cm^3, if the interface between the two layers is taken at 100 m. With $\tau_p = 2.5$ dynes/cm^2, the variation of w with distance offshore (calculated from Equation 13) is given in Table 3. In this case w is reduced by a factor of e^{-2} in 78 km; thus 78 km can be taken as the approximate breadth of the upwelling zone, as predicted by Yoshida's theory. The predicted average vertical speed in this zone is, from Table 3, about 6.5×10^{-3} cm/sec. In Cell 25, $\rho \doteq 1.0250$ gm/cm^3, $\Delta\rho \doteq 0.0020$ gm/cm^3, and $\tau_p = 5$ dynes/cm^2. This yields an upwelling zone 69 km wide with an average vertical speed, at 100 m, of 1.3×10^{-2} cm/sec (see Table 3).

Table 3. Vertical speeds at 100 m predicted by Yoshida's theory. x denotes distance offshore.

Cells 22 and 23		Cell 25	
x (km)	w (cm/sec)	x (km)	w (cm/sec)
10	1.2×10^{-2}	10	2.7×10^{-2}
20	0.96×10^{-2}	20	2.2×10^{-2}
40	0.57×10^{-2}	40	1.3×10^{-2}
60	0.34×10^{-2}	60	0.76×10^{-2}
80	0.20×10^{-2}	80	0.45×10^{-2}
100	0.12×10^{-2}	100	0.26×10^{-2}

These speeds and zone widths agree roughly with those given in Figure 11 for the inner upwelling band. This band borders the coast and is approximately 75 km wide. Its vertical speeds at 100 m are on the order of 10^{-2} cm/sec.

One would not, however, expect Equation 13 to hold across the broad, outer upwelling region of Figure 11. The equation is valid only for τ_p constant, whereas in the present case τ_p increased with distance offshore. The approximation τ_p = constant is acceptable in the narrow inner band (where the change in τ_p across the band is small) but not over the entire region.

A steady state has been assumed throughout. How reasonable is this assumption? The question is particularly appropriate in view of the yearly cycle of current reversals described above. The Southwest Monsoon generally begins in mid-May and continues through August. The winds are strongest during late June and July, when the Discovery data were taken. Since the data were gathered about a month and a half after the onset of the monsoon, the question to be answered is whether a month and a half is sufficient time for the ocean to adjust to a new wind regime.

Bryan (1963) investigated the response of a bounded, stratified ocean to a wind stress whose time variation consisted of a single step at $t = 0$. He found that the kinetic energy of the ocean, after an initial rise lasting less than a week, entered a series of damped

oscillations with a period of about 10 days. These had much less energy than the mean flow and appeared in many cases to reach negligible levels after a few cycles. Veronis and Stommel (1956) considered a similar wind stress acting on an unbounded stratified ocean. The response consisted of a steady wind-coupled flow, plus six waves. For the time and distance scales of the present problem, four of the waves can be disregarded: their energy would quickly be dispersed. The remaining two waves were a barotropic Rossby wave and a baroclinic Rossby wave, both in quasi-geostrophic equilibrium. The baroclinic wave would, in the present case, have a period of several years, and the associated accelerations would be negligibly small. The barotropic wave can be identified with the ten-day oscillation present in Bryan's model. Whether a month and a half is sufficient time for frictional forces to reduce this oscillation to negligible levels is not certain. In the present study it has been assumed that it is.

VII. SUMMARY AND CONCLUSIONS

The field of motion off the southeast coast of Arabia during the Southwest Monsoon has been examined, using a technique developed by Wyrtki (1963). The analysis was based on data obtained by R.R.S. Discovery in June and July of 1963, during the International Indian Ocean Expedition. Calculations were carried out with the aid of a computer program written especially for the study.

The numerical results are displayed in Figures 9, 11, 12, and 13. Figure 9 shows the absolute dynamic topography of the ocean surface south of the Arabian peninsula. The geostrophic flow is toward the northeast near shore, with indications of a southwestward countercurrent about 400 km offshore. Three large eddies are present, one of which (the westernmost) is also found during winter and appears to be permanent. The geostrophic velocities at the sea surface are mostly between 1/2 kt and 1 kt. To these must be added an offshore component of comparable magnitude caused by the wind stress.

Figures 11, 12, and 13 show mass transports between the ocean surface and 700 m. The wind-induced transport away from shore through the seaward perimeter of the region studied amounts to about 14 sv. This is balanced partly by motion toward shore at deeper levels, and partly by longshore flow toward the northeast, north of Socotra. Of these two sources, the latter is the more important.

From the calculated transports, it appears that upwelling along the Arabian coast is more extensive both horizontally and vertically than was previously supposed. During the Southwest Monsoon the winds are strong, steady, and nearly parallel to the coast. The wind stress increases with distance offshore, causing a divergence in the Ekman flow over an area some 1000 km long and at least 400 km wide. As a result, large quantities of water are carried away from shore in the surface layer. This water is supplied by strong upward motion over most of the region, down to depths of at least 700 m. Although the vertical extent of the upwelling is surprising (coastal upwelling elsewhere appears to be confined to the upper 100 or 200 m) it can be explained as a consequence of the unusual breadth of the upwelling zone.

BIBLIOGRAPHY

Bryan, K. 1963. A numerical investigation of a nonlinear model of a wind-driven ocean. Journal of the Atmospheric Sciences 20: 594-606.

Ramage, C. S. 1965. The summer atmospheric circulation over the Arabian Sea. Journal of the Atmospheric Sciences 23:144-150.

Rochford, D. J. 1964. Salinity maxima in the upper 1000 metres of the north Indian Ocean. Australian Journal of Marine and Freshwater Research 15:1-24.

_____ 1966. Source regions of oxygen maxima in intermediate depths of the Arabian Sea. Australian Journal of Marine and Freshwater Research 17:1-30.

Seryi, V. V. and V. Khimitsa. 1963. The hydrology and chemistry of the Gulf of Aden and the Arabian Sea. Okeanologiia 6:994-1003.

Smith, R. L. 1967. Note on Yoshida's (1955) theory of coastal upwelling. Journal of Geophysical Research 72:1396-1397.

Smith, R. L., J. G. Patullo and R. K. Lane. 1966. An investigation of the early stage of upwelling along the Oregon coast. Journal of Geophysical Research 71:1135-1140.

Stommel, H. M. 1956. On the determination of the depth of no meridional motion. Deep Sea Research 3:273-278.

_____ 1958. The Gulf Stream. Berkeley, University of California Press. 248 p.

Sverdrup, H. U. and R. H. Fleming. 1941. The waters off the coast of southern California, March to July, 1937. Bulletin of the Scripps Institution of Oceanography 4:261-378.

The Royal Society. 1963. International Indian Ocean Expedition, R. R. S. 'Discovery'. London. 24 p. (Cruise Report. Cruise 1. South East Arabian Upwelling Region)

Veronis, G. and H. M. Stommel. 1956. The action of variable wind stresses on a stratified ocean. Journal of Marine Research 15: 43-75.

Wyrtki, K. 1963. The horizontal and vertical field of motion in the Peru Current. Bulletin of the Scripps Institution of Oceanography 8:313-344.

APPENDIX

Appendix

The computer program described in Chapter V of this paper is coded in FORTRAN for the CDC 3300. A full listing is given below. Except for the use of REAL and INTEGER statements, the language of the program is at the level of FORTRAN II.

Figure 19 shows the main subdivisions of the data deck. The individual cards are described in Table 4. The first data card, the control card, contains three entries which are used principally in reading the remaining cards. The itinerary, which follows the control card, contains as many cards as there are cells to be analyzed. Each itinerary card describes a particular cell, and the order of the itinary cards determines the order in which the cells are taken up by the program. The first card is for Cell 1, the second is for Cell 2, and so on. As indicated in the text, a Type II cell may not be analyzed until all but one of its station heights have been determined.

An identification (ID) number is assigned to each station in the network. Although the ID numbers can be assigned in any order, they must run from 1 through NSTA, where NSTA is the total number of stations. That is, some one station of the network must have ID = 1, another must have ID = 2, and so on to ID = NSTA. Each itinerary card contains either three or four ID numbers, depending on whether the cell for that card has three or four sides. The ID

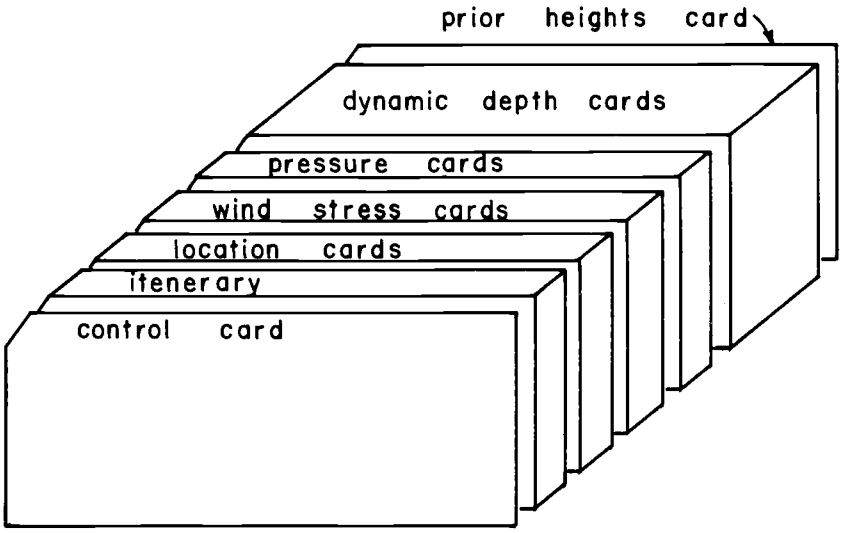

Figure 19. The data deck.

Table 4. Data card formats.

	Card columns	FORTRAN format	Internal name	Text symbol	Description
Control Card	1-10	I10	NCELLS	N	Total number of cells.
	11-20	I10	NSTA	-	Total number of stations.
	21-30	I10	MXNDPS	-	Maximum number of depths.
kth Itinerary Card	1-8	I8	KIND(k)	-	See Table 5.
	9	I1	SIDES(k)	m	Number of sides, kth cell (m = 3 or 4)
	10	I1	SEAL(k)	-	SEAL(k) = 0 produces free flow on all m sides of the kth cell. If SEAL(k) = q, the side between the qth and q + 1 st (mod m) stations of the cell is sealed at all depths; the remaining sides have free flow. SEAL(k) may not be greater than m.
	11-20	I10	ID(k, 1)	ID_{k1}	ID numbers of the stations of the kth cell, proceeding clockwise around the cell. If the cell has only 3 sides, the field for ID_{k4} is left blank.
	21-30	I10	ID(k, 2)	ID_{k2}	
	31-40	I10	ID(k, 3)	ID_{k3}	
	41-50	I10	ID(k, 4)	ID_{k4}	
	51-60	I10	NDPTHS(k)	-	Number of depths, kth cell. The pressure partition points for this cell are at $p = p^1, p^2, p^3, \ldots, p^r$ where r = NDPTHS(k) and $p^1 = 0$.
	61-70	I10	KNWNST(k)	-	Used only if KIND(k) = 3. KNWNST(k) = a, where ID(k, a) is the ID number of the station whose height is known before the kth cell is entered.

(Continued)

Table 4. (Continued).

	Card columns	FORTRAN format	Internal name	Text symbol	Description
jth Location Card	1-10	F10.0	LAT(4j-3)	-	Latitude, 4j-3 rd station (degrees). Positive N, negative S.
	11-20	F10.0	LONG(4j-3)	-	Longitude, 4j-3 rd station (degrees). Positive E, negative W.
	⋮	⋮	⋮	⋮	
	61-70	F10.0	LAT(4j)	-	Latitude, 4jth station (degrees).
	71-80	F10.0	LONG(4j)	-	Longitude, 4jth station (degrees).
jth Wind Stress Card	1-10	F10.0	TAU(4j-3)	τ_{4j-3}	Wind stress magnitude, 4j-3rd station (newtons/m).
	11-20	F10.0	WNDDIR (4j-3)	θ_{4j-3}	Compass point toward which $\vec{\tau}_{4j-3}$ is directed (degrees).
	⋮	⋮	⋮	⋮	
	61-70	F10.0	TAU(4j)	τ_{4j}	Wind stress magnitude, 4jth station (newtons/m).
	71-80	F10.0	WNDDIR(4j)	θ_{4j}	Compass point toward which $\vec{\tau}_{4j}$ is directed (degrees).
jth Pressure Card	1-10	F10.0	PRSR(8j-7)	p^{8j-7}	Pressure at 8j-7th isobaric surface (db).
	11-20	F10.0	PRSR(8j-6)	p^{8j-6}	Pressure at 8j-6th isobaric surface (db).
	⋮	⋮	⋮	⋮	
	71-80	F10.0	PRSR(8j)	p^{8j}	Pressure at 8jth isobaric surface (db).

(Continued)

Table 4. (Continued).

	Card columns	FORTRAN format	Internal name	Text symbol	Description
jth Dynamic Depth Card, ith Station	1-10	F10.0	DNDPTH (i, 8j-7)	D_i^{8j-7}	Dynamic depth or dynamic depth anomaly at the 8j-7th isobaric surface, ith station (dyn m).
	11-20	F10.0	DNDPTH (i, 8j-6)	D_i^{ij-6}	Dynamic depth or dynamic depth anomaly at the 8j-6th isobaric surface, ith station (dyn m).
	⋮	⋮	⋮	⋮	
	71-80	F10.0	DNDPTH (i, 8j)	D_i^{8j}	Dynamic depth or dynamic depth anomaly at the 8jth isobaric surface, ith station (dyn m).
Prior Heights Card	1-10	I10	I1	-	ID number of 1st station with known height.
	11-20	F10.0	Z(I1)	-	Height of 1st station with known height (dyn m).
	⋮	⋮	⋮	⋮	
	61-70	I10	I4	-	ID number of 4th station with known height.
	71-80	I10	Z(I4)	-	Height of 4th station with known height (dyn m).

Table 5. Explanation of KIND(k).

Value of KIND(k)	Meaning
1	Cell k is a Type I cell, and the prior heights card is empty. Used only for k = 1. All station heights in the network will be computed relative to the 1st station of Cell 1. Example: Cell 1 of Figures 6a and 6b.
2	Cell k is a Type I cell, and the heights of the 1st and 2nd stations of the cell are known before it is entered. The height of the 1st station will not be changed, but the final height of the 2nd station will be an average of the new height, given no change in that of the 1st station, and the prior height. Used for cells like Cell 2 of Figure 6a, where B and G are the 1st and 2nd stations of the cell.
3	Cell k is a Type I cell, and the height of the jth station of the cell (the station with ID = ID(k, j)) is known before the cell is entered, where j = KNWNST(k).
4	Cell k is a Type II cell. All but one of its station heights are known when the cell is entered.

numbers are placed on the card in the order in which an observer moving clockwise around the cell would encounter the stations to which they correspond. If the cell is a Type II cell, the number of the "new" station (whose height is to be determined) must be the second ID number on the card.

The location cards specify the latitude and longitude of each station. These numbers are placed on the cards in pairs, four pairs to a card, starting with the station having ID = 1 and proceeding in order by ID number. If NSTA is not an integral multiple of 4, the last location card will contain fewer than four pairs of entries.

Wind stresses are treated in the same way. Every wind stress card (except, possibly, the last) contains four pairs of numbers for four stations. Each pair consists of a stress magnitude (τ) and its direction (θ). The pairs are ordered by station ID number.

The pressure cards contain the numbers p^j, $j=1,2,\ldots,$MXNDPS. $p^1 = 0$ always, and $p^{i+1} > p^i$. These numbers are punched eight to a card, except possibly for the last pressure card, which will have eight entries only if MXNDPS is evenly divisible by eight.

Dynamic depth anomalies are read into the computer on dynamic depth cards. The number of anomalies input for each station depends on the depths of the cells that contain the station. Suppose, for example, that a particular station lies on the perimeters of several adjoining cells (like Station F of Figure 4), the deepest of which has

$p_b = p^r$ where $r \leq$ MXNDPS. The dynamic depth cards for this station will contain depth anomalies[10] for the pressure surfaces $p = p^1, p^2, \ldots, p^r$. These numbers are punched eight to a card, starting with p^1 and ending with p^r. The cards for Station 1 are first, followed by those for Station 2, followed by those for Station 3, and so on. The card set for each station must contain exactly MXNDPS/8 cards if MXNDPS/8 is an integer, and [MXNDPS/8 + 1] cards otherwise, where $[\cdot]$ denotes rounding to the next lower integer. If MXNDPS is not evenly divisible by 8, the last card of each set will have empty fields. Indeed, if MXNDPS - $r \geq 8$ for a given station, the last card for that station will have no entries at all. If MXNDPS - $r \geq 16$, the last <u>two</u> cards of the set will be empty. This is inefficient in terms of cards used, but leads to greater efficiency in the logic of the program.

The last card of the set is the <u>prior heights</u> card. This card is always included but is left blank unless two or more station heights are known from prior considerations. Up to four heights can be specified in this way. As an example, suppose that current measurements indicate that Station 16 of the network is 6.9 dynamic cm lower than Station 12, and 2.3 dynamic cm higher than Station 17. This information would be input to the computer by punching I1 = 16, Z(I1) = 0,

---

[10] Dynamic depths can be used in lieu of anomalies, if depths rather than anomalies are available.

I2 = 12, Z(I2) = 0. 060, I3 = 17, and Z(I3) = -0. 023 on the prior heights card. The heights of the remaining stations of the network would then be computed relative to Station 16. In a case of this sort, a tuning cell would not be required; that is, the network could (and ordinarily would) consist entirely of Type II cells.

The reader will note from Table 4 that all of the physical inputs must be dimensioned in the MTS system. The numerical outputs are also given in MTS units.

PROGRAM LISTING

```
      PROGRAM CNTROL
C     THE PROGRAM IS DIMENSIONED FOR 50 STATIONS, 45 CELLS, AND 40 DEPTHS.
      DIMENSION Z(50), DNDPTH(50,40), WNDDIR(50), TAU(50),
     X  PRSR(40), ID(45, 4), LAT(50), LONG(50), NDPTHS(45),
     X  KNWNST(45), VRLNM(4,40), EL(4), KIND(45), SIDES(45), SEAL(45)
      COMMON Z, DNDPTH, WNDDIR, TAU, PRSR, ID, K, LAT, LONG,
     X  NDPTHS, NDPS, VRLNM, EL, KIND, SIDES, SEAL, KNWNST
      REAL LAT, LONG
      INTEGER SIDES, SEAL
   10 FORMAT (3I10)
   15 FORMAT (I8, 2I1, 6I10)
   20 FORMAT (8F10.0)
      READ 10, NCELLS, NSTA, MXNDPS
      READ 15, (KIND(K), SIDES(K), SEAL(K), (ID(K,L), L = 1, 4),
     X  NDPTHS(K), KNWNST(K), K = 1, NCELLS)
C     READ LATITUDE AND LONGITUDE AT EACH STATION.  LAT IS + IN N
C     HEMISPHERE AND - IN S HEMISPHERE. LONG IS + E OF GREENWICH AND -
C     W OF GREENWICH.
      READ 20, (LAT(I), LONG(I), I = 1, NSTA)
C     READ MAGNITUDE AND DIRECTION OF WINDSTRESS AT EACH STATION.
C     WNDDIR IS THE DIRECTION TOWARD WHICH THE WIND IS BLOWING.
      READ 20, (TAU(I), WNDDIR(I), I = 1, NSTA)
C     READ THE PRESSURES, IN DECIBARS, OF THE PARTITION POINTS.
      READ 20,    (PRSR(J), J = 1, MXNDPS)
C     READ THE DYNAMIC DEPTH ANOMALIES.
      DO 30 I = 1, NSTA
   30 READ 20,    (DNDPTH(I,J), J = 1, MXNDPS)
C     READ UP TO 4 KNOWN STATION HEIGHTS.
      READ 35, I1, Z(I1), I2, Z(I2), I3, Z(I3), I4, Z(I4)
   35 FORMAT (4(I10, F10.0))
      DO 40 I = 1, NSTA
      LAT(I) = LAT(I)/57.295779
      LONG(I) = LONG(I)/57.295779
   40 WNDDIR(I) = WNDDIR(I)/57.295779
C     PROCEED TO THE FIRST PRISM (K DENOTES CELL NUMBER).
      K = 1
   50 IF (KIND(K) - 3) 100, 100, 200
  100 CALL PRISM1
C     THIS CELL IS A TYPE I (OR TUNING) CELL.
  110 K = K + 1
      IF (K - NCELLS) 50, 50, 700
  200 CALL PRISM2
C     THIS CELL IS A TYPE II CELL.
      GO TO 110
  700 DO 705 I = 1, NSTA
      LAT(I) = LAT(I)*57.295779
  705 LONG(I) = LONG(I)*57.295779
      PRINT 710, (I, LAT(I), LONG(I), Z(I), I = 1, NSTA)
  710 FORMAT (1H1, 9X, 40HSUMMARY OF STATION POSITIONS AND HEIGHTS///
     X  15X, 7HSTATION, 6X, 3HLAT, 8X, 4HLONG, 5X, 9HH (DYN M)//
     X  (I19, F13.3, F12.3, F12.6))
      STOP
      END
```

```
      SUBROUTINE PRISM1
C     TUNING PRISM
      DIMENSION LAT(50), LONG(50), Z(50), ZZ(4), DNDPTH(50,40),
     X  PRSR(40), ID(45,4), DNDP(4,40), VRLNM(4,40), DDLNM(4),
     X  EL(4), TAU(50), WNDDIR(50), EKMAS(4), VREF(4), VRS(4,40),
     X  TAUCMP(4), F(4), NDPTHS(45), TOTMAS(40), KIND(45), SIDES(45),
     X  SEAL(45), KNWNST(45)
      COMMON Z, DNDPTH, WNDDIR, TAU, PRSR, ID, K, LAT, LONG,
     X  NDPTHS, NDPS, VRLNM, EL, KIND, SIDES, SEAL, KNWNST
      REAL LAT, LONG
      INTEGER FLAG, SIDES, SEAL
      IEND = SIDES(K)
      NDPS = NDPTHS(K)
      DO 30 I = 1, IEND
      L = ID(K,I)
      DO 30 J = 1, NDPS
   30 DNDP(I,J) = DNDPTH(L,J)
C     COMPUTE THE LENGTH OF EACH SIDE OF THE CELL, THE EKMAN
C     TRANSPORT THROUGH IT, AND THE VELOCITY RELATIVE TO THE SURFACE
C     AT EACH OF THE NDPS PRESSURE SURFACES.
      DO 62 I = 1, IEND
      L1 = ID(K,I)
      IF (I - IEND) 42, 40, 40
   40 II = 1
      GO TO 44
   42 II = I + 1
   44 L2 = ID(K,II)
      F(I) = 0.0000729*(SIN(LAT(L1)) + SIN(LAT(L2)))
      DXSTN = 3185615.0*(LONG(L2) - LONG(L1))*(COS(LAT(L1)) +
     X  COS(LAT(L2)))
      DYSTN = 6371230.0*(LAT(L2) - LAT(L1))
      EL(I) = SQRT(DXSTN**2 + DYSTN**2)
      DXTAU = 0.5*(TAU(L1)*SIN (WNDDIR(L1))+TAU(L2)*SIN (WNDDIR(L2)))
      DYTAU = 0.5*(TAU(L1)*COS (WNDDIR(L1))+TAU(L2)*COS (WNDDIR(L2)))
      TAUCMP(I) = (DXTAU*DXSTN + DYTAU*DYSTN)/EL(I)
      IF (SEAL(K) - I) 54, 50, 54
   50 EKMAS(I) = 0.
      DO 52 J = 1, NDPS
   52 VRS(I,J) = 0.
      GO TO 62
   54 EKMAS(I) = 0.001*TAUCMP(I)*EL(I)/F(I)
      Q = 10.0/(F(I)*EL(I))
      DO 60 J = 1, NDPS
   60 VRS(I,J) = Q*(DNDP(II,J) - DNDP(I,J))
      VREF(I) = VRS(I,NDPS)
   62 CONTINUE
      M = NDPS
      FLAG = 0
   70 TOTMAS(M) = 0.
      DO 100 I = 1, IEND
      IF (SEAL(K) - I) 78, 100, 78
C     COMPUTE THE SPEED RELATIVE TO THE PRESENT LAYER OF NO MOTION.
   78 DO 80 J = 1, NDPS
   80 VRLNM(I,J) = VRS(I,J) - VREF(I)
      NDEPM1 = NDPS - 1
      GEOMAS = 0.
      DO 90 J = 1, NDEPM1
      VBAR = 0.5*(VRLNM(I,J) + VRLNM(I,J+1))
```

```
      DP = PRSR(J+1) - PRSR(J)
   90 GEOMAS = GEOMAS + DP*EL(I)*VBAR/0.98
      TOTMAS(M) = TOTMAS(M) + GEOMAS + EKMAS(I)
  100 CONTINUE
      IF (FLAG) 112, 112, 115
  112 M = M - 1
C     M IS THE NUMBER OF THE LEVEL JUST ABOVE THE LEVEL JUST TRIED.
      IF (M) 400, 400, 113
  113 DO 114 I = 1, IEND
  114 VREF(I) = VRS(I, M)
C     MOVE UPWARD ONE WHOLE LAYER.
      OLDMAS = TOTMAS(M+1)
      FLAG = FLAG + 1
      GO TO 70
  115 IF (OLDMAS*TOTMAS(M)) 120, 120, 112
C     IF THE TOTAL TRANSPORT HAS CHANGED SIGN, WE HAVE JUST PASSED
C     THE LAYER OF NO MOTION.
  120 FRAC = 1./(1. - OLDMAS/TOTMAS(M))
      PLNM = PRSR(M) + FRAC*(PRSR(M+1) - PRSR(M))
      DO 130 I = 1, IEND
      VREF(I) = VRS(I,M) + FRAC*(VRS(I,M+1) - VRS(I,M))
      DO 130 J = 1, NDPS
  130 VRLNM(I,J) = VRS(I,J) - VREF(I)
C     COMPUTE THE DYNAMIC DEPTH ANOMALY AT THE LNM, FOR EACH STATION,
C     AND THE HEIGHT OF EACH STATION RELATIVE TO THE FIRST
      DO 210 I = 1, IEND
      DDLNM(I) = DNDP(I,M) + FRAC*(DNDP(I,M+1) - DNDP(I,M))
  210 ZZ(I) = DDLNM(I) - DDLNM(1)
      IF (KIND(K) - 1) 220, 220, 224
  220 DO 222 I = 1, IEND
      L = ID(K, I)
  222 Z(L) = ZZ(I)
      GO TO 232
  224 IF (KIND(K) - 2) 226, 226, 228
  226 ID1 = ID(K,1)
      ID2 = ID(K,2)
      ID3 = ID(K,3)
      ID4 = ID(K,4)
      Z(ID2) = .5*(Z(ID2) + Z(ID1) + ZZ(2))
      Z(ID3) = Z(ID1) + ZZ(3)
      Z(ID4) = Z(ID1) + ZZ(4)
      GO TO 232
  228 M1 = KNWNST(K)
      M2 = ID(K, M1)
      DO 230 I = 1, IEND
      L = ID(K,I)
  230 Z(L) = Z(M2) + ZZ(I) - ZZ(M1)
  232 PRINT 300, K, (ID(K,I), I = 1, IEND)
      L1 = ID(K,1)
      L2 = ID(K,2)
      L3 = ID(K,3)
      IF (SIDES(K) - 3) 236, 236, 234
  234 L4 = ID(K,4)
      PRINT 306, Z(L1), Z(L2), Z(L3), Z(L4)
      PRINT 312
      GO TO 248
  236 PRINT 306, Z(L1), Z(L2), Z(L3)
      PRINT 310
  248 DO 250 J = 1, NDPS
```

```
250 PRINT 320, PRSR(J), (VRS(I,J), I = 1, IEND)
    IF (SIDES(K) - 3) 252, 252, 254
252 PRINT 315
    GO TO 256
254 PRINT 317
256 DO 260 J = 1, NDPS
260 PRINT 320, PRSR(J), (VRLNM(I,J), I = 1, IEND)
    PRINT 330, (EL(I), I = 1, IEND)
    PRINT 335, (TAUCMP(I), I = 1, IEND)
    PRINT 340, (EKMAS(I), I = 1, IEND)
    PRINT 342
    PRINT 345, (F(I), I = 1, IEND)
    PRINT 350, PLNM
300 FORMAT (1H1, 9X, 11HCELL NUMBER, I3///10X, 7HSTATION, 17X, I2,
   X  11X, I2, 11X, I2, 11X, I2)
304 FORMAT (/10X, 14HHEIGHT (DYN M), F15.6, 3F13.6)
310 FORMAT (///10X,
   X  54HGEOSTROPHIC VELOCITIES RELATIVE TO THE SURFACE (M/SEC)//15X,
   X  9HPRSR (DB), 10X, 6HSIDE 1, 10X, 6HSIDE 2, 10X, 6HSIDE 3/)
312 FORMAT (///10X,
   X  54HGEOSTROPHIC VELOCITIES RELATIVE TO THE SURFACE (M/SEC)//15X,
   X  9HPRSR (DB), 10X, 6HSIDE 1, 10X, 6HSIDE 2, 10X, 6HSIDE 3,
   X  10X, 6HSIDE 4/)
315 FORMAT (///10X,
   X  39HABSOLUTE GEOSTROPHIC VELOCITIES (M/SEC)//15X,
   X  9HPRSR (DB), 10X, 6HSIDE 1, 10X, 6HSIDE 2, 10X, 6HSIDE 3/)
317 FORMAT (///10X,
   X  39HABSOLUTE GEOSTROPHIC VELOCITIES (M/SEC)//15X,
   X  9HPRSR (DB), 10X, 6HSIDE 1, 10X, 6HSIDE 2, 10X, 6HSIDE 3,
   X  10X, 6HSIDE 4/)
320 FORMAT (F20.0, 4X, 4F16.6)
330 FORMAT (//10X, 10HLENGTH (M), F19.1, 3F16.1)
335 FORMAT (/10X, 11HTAU (N/SQM), F18.5, 3F16.5)
340 FORMAT (/10X, 11HEKMAN XPORT, F18.1, 3F16.1)
342 FORMAT (11X, 10H(TONS/SEC))
345 FORMAT (/10X, 8HF (/SEC), F21.10, 3F16.10)
350 FORMAT (///10X, 20HPRESSURE AT LNM (DB), F12.1)
    CALL TRANSP
    RETURN
400 PRINT 410
410 FORMAT (1H1, 10X, 34HCOULD NOT FIND LNM IN TUNING PRISM )
    IF (SIDES(K) - 3) 412, 412, 414
412 PRINT 310
    GO TO 416
414 PRINT 312
416 DO 420 J = 1, NDPS
420 PRINT 320, PRSR(J), (VRS(I,J), I = 1, IEND)
    PRINT 430
430 FORMAT (///10X, 39HNET MASS TRANSPORT AS A FUNCTION OF LNM///
   X  15X, 9HPRSR (DB), 5X, 20HTRANSPORT (TONS/SEC)//)
    M = NDPS
440 PRINT 450, PRSR(M), TOTMAS(M)
450 FORMAT (F21.0, F22.1)
    M = M - 1
    IF (M) 460, 460, 440
460 CALL EXIT
    END
```

```
      SUBROUTINE PRISM2
C     TYPE II CELL.
      DIMENSION Z(50), DNDPTH(50,40), PRSR(40), ID(45,4),
     X  LAT(50), LONG(50), TAU(50), WNDDIR(50), VRS(4,40), DNDP(4,40),
     X  VRLNM(4,40), F(4), EL(4), TAUCMP(4), EKMAS(4), DH(4), PLNM(4),
     X  VSLOPE(4), NDPTHS(45), KIND(45), SIDES(45), SEAL(45), KNWNST(45)
      COMMON Z, DNDPTH, WNDDIR, TAU, PRSR, ID, K, LAT, LONG,
     X  NDPTHS, NDPS, VRLNM, EL, KIND, SIDES, SEAL, KNWNST
      REAL LAT, LONG
      INTEGER SIDES, SEAL
      NDPS = NDPTHS(K)
      IEND = SIDES(K)
      DO 30 I = 1, IEND
      L = ID(K,I)
      DO 30 J = 1, NDPS
   30 DNDP(I,J) = DNDPTH(L,J)
      RLTOTL = 0.
      EKTOTL = 0.
      DO 62 I = 1, IEND
      L1 = ID(K,I)
      IF (I - IEND) 42, 40, 40
   40 II = 1
      GO TO 44
   42 II = I + 1
   44 L2 = ID(K,II)
C     COMPUTE THE AVERAGE VALUE OF THE CORIOLIS PARAMETER ALONG THE ITH
C     SIDE, AND THE LENGTH OF THE ITH SIDE.
      F(I) = 0.0000729*(SIN(LAT(L1)) + SIN(LAT(L2)))
      DXSTN = 3185615.0*(LONG(L2) - LONG(L1))*(COS(LAT(L1)) +
     X  COS(LAT(L2)))
      DYSTN = 6371230.0*(LAT(L2) - LAT(L1))
      EL(I) = SQRT(DXSTN**2 + DYSTN**2)
C     COMPUTE THE COMPONENT OF TAU ALONG THE ITH SIDE.
      DXTAU = 0.5*(TAU(L1)*SIN (WNDDIR(L1)) + TAU(L2)*SIN (WNDDIR(L2)))
      DYTAU = 0.5*(TAU(L1)*COS (WNDDIR(L1)) + TAU(L2)*COS (WNDDIR(L2)))
      TAUCMP(I) = (DXTAU*DXSTN + DYTAU*DYSTN)/EL(I)
      IF (SEAL(K) - I) 54, 50, 54
   50 EKMAS(I) = 0.
      DO 52 J = 1, NDPS
   52 VRS(I,J) = 0.
      GO TO 62
   54 EKMAS(I) = 0.001*TAUCMP(I)*EL(I)/F(I)
      Q = 10.0/(F(I)*EL(I))
      SUM = 0.
      VRS(I,1) = 0.
      DO 56 J = 2, NDPS
      VRS(I,J) = Q*(DNDP(II,J) - DNDP(I,J))
      VBAR = 0.5*(VRS(I,J-1) + VRS(I,J))
   56 SUM = SUM + VBAR*(PRSR(J) - PRSR(J-1))
      RLTOTL = RLTOTL + SUM*EL(I)/0.98
      EKTOTL = EKTOTL + EKMAS(I)
   62 CONTINUE
C     COMPUTE Z(L2), THE ABSOLUTE HEIGHT OF THE 2ND STATION OF THE
C     CELL, IN DYNAMIC METERS, REFERENCED TO THE 1ST STATION OF THE
C     INITIAL TUNING CELL, OR TO THE 1ST INPUT STATION.
      L1 = ID(K,1)
      L2 = ID(K,2)
      L3 = ID(K,3)
```

```
      IF (SIDES(K) - 3) 63, 63, 70
   63 DH(3) = (Z(L1) - Z(L3))/0.98
      B1 = -DH(3)
      B2 = -DH(3)/F(3) + (RLTOTL + EKTOTL)/(10.0*PRSR(NDPS))
      IJK = SEAL(K) + 1
      GO TO (64, 65, 66, 67), IJK
   64 DH(1) = (B1/F(2) - B2)/(1./F(2) - 1./F(1))
      GO TO 68
   65 DH(1) = B1 - B2*F(2)
      GO TO 68
   66 DH(1) = B2*F(1)
      GO TO 68
   67 B2 = B2 + DH(3)/F(3)
      GO TO 64
   68 DH(2) = -DH(1) - DH(3)
      GO TO 79
   70 L4 = ID(K,4)
      DH(3) = (Z(L4) - Z(L3))/0.98
      DH(4) = (Z(L1) - Z(L4))/0.98
      B1 = -DH(3) - DH(4)
      B2 = -DH(3)/F(3) -DH(4)/F(4) + (RLTOTL + EKTOTL)/(10.0*PRSR(NDPS))
      IJK = SEAL(K) + 1
      GO TO (71, 72, 73, 74, 75), IJK
   71 DH(1) = (B1/F(2) - B2)/(1./F(2) - 1./F(1))
      GO TO 76
   72 DH(1) = B1 - B2*F(2)
      GO TO 76
   73 DH(1) = B2*F(1)
      GO TO 76
   74 B2 = B2 + DH(3)/F(3)
      GO TO 71
   75 B2 = B2 + DH(4)/F(4)
      GO TO 71
   76 DH(2) = -DH(1) - DH(3) - DH(4)
   79 Z(L2) = Z(L1) + DH(1)*0.98
C     ADD THE SLOPE VELOCITIES TO THE RELATIVE VELOCITIES, AND FIND THE
C     PRESSURE SURFACE WHERE THE TOTAL VELOCITY IS ZERO.  THE LNM WILL
C     IN GENERAL BE DIFFERENT ON DIFFERENT SIDES.
      DO 90 I = 1, IEND
      IF (SEAL(K) - I) 84, 82, 84
   82 VSLOPE(I) = 0.
      GO TO 86
   84 VSLOPE(I) = -9.8*DH(I)/(EL(I)*F(I))
   86 DO 90 J = 1, NDPS
   90 VRLNM(I,J) = VRS(I,J) + VSLOPE(I)
      PRINT 300, K, (ID(K,I), I = 1, IEND)
      L1 = ID(K,1)
      L2 = ID(K,2)
      L3 = ID(K,3)
      IF (SIDES(K) - 3) 236, 236, 234
  234 L4 = ID(K,4)
      PRINT 306, Z(L1), Z(L2), Z(L3), Z(L4)
      PRINT 312
      GO TO 248
  236 PRINT 306, Z(L1), Z(L2), Z(L3)
      PRINT 310
  248 DO 250 J = 1, NDPS
  250 PRINT 320, PRSR(J), (VRS(I,J), I = 1, IEND)
      IF (SIDES(K) - 3) 252, 252, 254
```

```
252 PRINT 315
    GO TO 256
254 PRINT 317
256 DO 260 J = 1, NDPS
260 PRINT 320, PRSR(J), (VRLNM(I,J), I = 1, IEND)
    PRINT 330, (EL(I), I = 1, IEND)
    PRINT 335, (TAUCMP(I), I = 1, IEND)
    PRINT 340, (EKMAS(I), I = 1, IEND)
    PRINT 342
    PRINT 345, (F(I), I = 1, IEND)
300 FORMAT (1H1, 9X, 11HCELL NUMBER, I3///10X, 7HSTATION, 17X, I2,
   X  11X, I2, 11X, I2, 11X, I2)
306 FORMAT (/10X, 14HHEIGHT (DYN M), F15.6, 3F13.6)
310 FORMAT (///10X,
   X  54HGEOSTROPHIC VELOCITIES RELATIVE TO THE SURFACE (M/SEC)//15X,
   X  9HPRSR (DB), 10X, 6HSIDE 1, 10X, 6HSIDE 2, 10X, 6HSIDE 3/)
312 FORMAT (///10X,
   X  54HGEOSTROPHIC VELOCITIES RELATIVE TO THE SURFACE (M/SEC)//15X,
   X  9HPRSR (DB), 10X, 6HSIDE 1, 10X, 6HSIDE 2, 10X, 6HSIDE 3,
   X  10X, 6HSIDE 4/)
315 FORMAT (///10X,
   X  39HABSOLUTE GEOSTROPHIC VELOCITIES (M/SEC)//15X,
   X  9HPRSR (DB), 10X, 6HSIDE 1, 10X, 6HSIDE 2, 10X, 6HSIDE 3/)
317 FORMAT (///10X,
   X  39HABSOLUTE GEOSTROPHIC VELOCITIES (M/SEC)//15X,
   X  9HPRSR (DB), 10X, 6HSIDE 1, 10X, 6HSIDE 2, 10X, 6HSIDE 3,
   X  10X, 6HSIDE 4/)
320 FORMAT (F20.0, 4X, 4F16.6)
330 FORMAT (//10X, 10HLENGTH (M), F19.1, 3F16.1)
335 FORMAT (/10X, 11HTAU (N/SQM), F18.5, 3F16.5)
340 FORMAT (/10X, 11HEKMAN XPORT, F18.1, 3F16.1)
342 FORMAT (11X, 10H(TONS/SEC))
345 FORMAT (/10X, 8HF (/SEC), F21.10, 3F16.10)
    CALL TRANSP
    RETURN
    END


    SUBROUTINE TRANSP
    DIMENSION Z(50), DNDPTH(50,40), WNDDIR(50), TAU(50),
   X  PRSR(40), ID(45,4), LAT(50), LONG(50), NDPTHS(45), KIND(45),
   X  VRLNM(4,40), EL(4), TRNS1(4,40), STRNS1(40), TRNS2(4), SEAL(45),
   X  SIDES(45), KNWNST(45)
    COMMON Z, DNDPTH, WNDDIR, TAU, PRSR, ID, K, LAT, LONG,
   X  NDPTHS, NDPS, VRLNM, EL, KIND, SIDES, SEAL, KNWNST
    REAL LAT, LONG
    INTEGER SIDES, SEAL
  4 FORMAT (1H1, 9X, 36HGEOSTROPHIC MASS TRANSPORTS FOR CELL, I3,
   X  11H (TONS/SEC)/// 12X, 8HPRESSURE, 10X, 6HSIDE 1, 10X, 6HSIDE 2,
   X  10X, 6HSIDE 3, 10X, 10HNET INFLUX / 14X, 4H(DB) //)
  6 FORMAT (1H1, 9X, 36HGEOSTROPHIC MASS TRANSPORTS FOR CELL, I3,
   X  11H (TONS/SEC)/// 12X, 8HPRESSURE, 10X, 6HSIDE 1, 10X, 6HSIDE 2,
   X  10X, 6HSIDE 3, 10X, 6HSIDE 4, 10X, 10HNET INFLUX / 14X, 4H(DB)
   X  //)
  8 FORMAT (9X, F5.0, 1X, 2HTO, F5.0, F15.1, 2F16.1, F17.1)
 10 FORMAT (9X, F5.0, 1X, 2HTO, F5.0, F15.1, 3F16.1, F17.1)
    IEND = SIDES(K)
    ISIDES = SIDES(K) - 2
    GO TO (20, 22), ISIDES
```

```
 20 PRINT 4, K
    GO TO 35
 22 PRINT 6, K
 35 DO 50 J = 2, NDPS
    DZ = (PRSR(J) - PRSR(J-1))/0.98
    STRNS1(J-1) = 0.
    DO 40 I = 1, IEND
    VBAR = 0.5*(VRLNM(I,J-1) + VRLNM(I,J))
    TRNS1(I,J-1) = VBAR*DZ*EL(I)
 40 STRNS1(J-1) = STRNS1(J-1) + TRNS1(I,J-1)
    GO TO (42, 44), ISIDES
 42 PRINT 8, PRSR(J-1), PRSR(J), (TRNS1(I,J-1), I = 1, 3), STRNS1(J-1)
    GO TO 50
 44 PRINT 10, PRSR(J-1), PRSR(J), (TRNS1(I,J-1), I = 1, 4),
   X  STRNS1(J-1)
 50 CONTINUE
    PRINT 60
 60 FORMAT (///)
    INDIC = 0
    J1 = 1
    J2 = 6
 65 STRNS2 = 0.
    DO 80 I = 1, IEND
    TRNS2(I) = 0.
    DO 70 J = J1, J2
 70 TRNS2(I) = TRNS2(I) + TRNS1(I,J)
 80 STRNS2 = STRNS2 + TRNS2(I)
    GO TO (82, 84), ISIDES
 82 PRINT 8, PRSR(J1), PRSR(J2+1), (TRNS2(I), I = 1, 3), STRNS2
    GO TO 90
 84 PRINT 10, PRSR(J1), PRSR(J2+1), (TRNS2(I), I = 1, 4), STRNS2
 90 INDIC = INDIC + 1
    GO TO (95, 100, 105, 120, 200), INDIC
 95 J1 = 7
    J2 = 10
    GO TO 65
100 J1 = 11
    J2 = 18
    GO TO 65
105 IF (NDPS - 24) 115, 110, 110
110 J1 = 19
    J2 = 23
    GO TO 65
115 J1 = 19
    J2 = NDPS - 1
    GO TO 65
120 IF (NDPS - 24) 200, 200, 125
125 J1 = 24
    J2 = NDPS - 1
    GO TO 65
200 RETURN
    END
```